IPK INTERNATIONAL INC.

# FINAL REPORT

## FIELD TRIAL & CHARACTERIZATION OF A LOW-HEAD PHOTOVOLTAIC POWERED PUMPING SYSTEM

BY:

C.E. Norman

(DSS File No. 55SZ.23216-6-6110)

January, 1988

T3-W6
88-6110

36 BENTLEY AVENUE, NEPEAN, ONTARIO, CANADA K2E 6T8
TEL:(613)225-4403 Tlx: 053-3930

89-05646/

## SUMMARY

**TITLE:** FINAL REPORT ON FIELD TRIAL AND CHARACTERIZATION OF A LOW-HEAD PHOTOVOLTAIC POWERED PUMPING SYSTEM


**CONTRACTOR:**
TPK International Inc.
36 Bentley Avenue
Nepean, Ontario
K2E 6T8

**SCIENTIFIC AUTHORITY:**
Mr. J. Larry McClung
Renewable Energy Division
Energy, Mines & Resources
460 O'Connor Street
Ottawa, Ontario
K1A 0E4

**PRINCIPAL INVESTIGATOR:**
C.E. Norman, Ph.D.
(613)225-4403



**CONTRACT NO.:**
23216-6-6110/-1-SZ
(DSS File #55SZ.23216-6-6110)

**DURATION:** 19 Months
(JULY 1986 - JAN. 1988)

**COST:** Total $ 65,433.01
(Crown Contribution: $ 48,497.74
Fiscal Year 1986/87, 1987/88



**OBJECTIVES:**

To design a PV system to pump 60 $m^3$/day at a static head of 7 m. To characterize the components and system in the laboratory. To develop a PV powered data acquisition system for the pump. To subject both to a four month field trial and then re-test and evaluate the pump system.

**RESULTS:**

In laboratory tests, the pump system functioned as designed, with a peak efficiency over 50% and good matching between components. The monitoring instruments and data loggers had several initial problems but functioned adequately. In the field trial, the pump operated reliably but at slightly reduced efficiency, traceable to increased friction due to grease on the pump seal.

**CONCLUSIONS:**

Correcting for the seal friction problem, the pump system met the design specifications. The field trial provided considerable experience in pump installation and operation, and demonstrated the reliability of the system.

# FINAL REPORT
# ON
# FIELD TRIAL AND CHARACTERIZATION OF A LOW-HEAD PHOTOVOLTAIC POWERED PUMPING SYSTEM

**RENEWABLE ENERGY DIVISION**

**PREPARED FOR:**

Renewable Energy Division
Coal and Alternative Energy Branch
Energy, Mines and Resources Canada
Ottawa, Canada
DSS Contract File No.: 55SZ.23216-6-6110

January, 1988

**PREPARED BY:**

C.E. Norman
TPK International Inc.
36 Bentley Avenue
Nepean, Ontario
K2E 6T8
Phone: (613) 225-4403

**SCIENTIFIC AUTHORITY:**

Mr. J. Larry McClung
Technology Coordinator, Photovoltaics
Solar Energy Development Program
Renewable Energy Division
Energy, Mines and Resources Canada

This report is distributed for informational purposes only and does not necessarily reflect the views of the Government of Canada nor constitute an endorsement of any commercial product or person. Neither Canada nor its ministers, officers, employees or agents makes any warranty in respect of this report or assumes any liability arising out of this report.

## RESTRICTIONS ON DISCLOSURE

The design concepts, prototypes, test techniques and results described in this report are confidential. As such, they shall not be disclosed outside Energy, Mines and Resources Canada or be duplicated in whole or in part without the express, written consent of an authorized officer of TPK International Inc. for a period of 12 months. This restriction does not limit the Crown's right to use information contained in this report if it is obtained from another source.

## TABLE OF CONTENTS


| | | |
|---|---|---|
| | Acknowledgements | i |
| | Preface | ii |
| | Abstract | iii |
| | Executive Summary | iv |
| | Resume | vii |
| 1.0 | INTRODUCTION | 1 |
| 2.0 | SYSTEM DESIGN | 3 |
| 3.0 | DATA ACQUISITION SYSTEM | 6 |
| 4.0 | LABORATORY TESTING OF SYSTEM COMPONENTS | 10 |
| 5.0 | OUTDOOR TESTING | 14 |
| 6.0 | ANALYSIS AND EVALUATION | 17 |
| 7.0 | FIELD INSTALLATION | 21 |
| 8.0 | FIELD RESULTS | 23 |
| 9.0 | EVALUATION AND DISCUSSION | 27 |
| 10.0 | CONCLUSIONS AND RECOMMENDATIONS | 29 |
| | REFERENCES | 31 |
| | APPENDIX A: FIGURES AND TABLES | 33 |

## ACKNOWLEDGEMENTS

The author would like to thank Anne Campbell of Almonte, Ontario for the use of her water front and yard as the site for the field trial, and for courtesies shown TPK employees visiting the site. In addition, the author wishes to acknowledge those at TPK who helped make this project a success: Raye Thomas, for project coordination and technical advice, Albino Genovesse, Victor Breault, Gianfranco Petrilli and Dave Mather for their assistance with the pump installation, laboratory testing and data logging, and Jenny Hull for her administrative help.

Funding for this project was provided by the Panel of Energy Research and Development, Office of Energy Research and Development, Energy, Mines and Resources Canada.

Norman, C.E., TPK International Inc. Field Trial and Characterization of a Low-Head Photovoltaic Powered Pumping System. Report of Contract File # 55SZ.23216-6-6110. Renewable Energy Division, Energy, Mines and Resources Canada, Ottawa, Ontario. 1987. (71 pp.)

Copies of this report may be obtained through:

Renewable Energy Division
Energy, Mines & Resources Canada
580 Booth Street
Ottawa, Ontario
K1A 0E4

(613) 995-9447

OR

Interlibrary Loans
CISTI Library
National Research Council
Bldg. M-55, Montreal Road
Ottawa, Ontario
K1A 0S2
(613) 993-1585

## PREFACE

This report describes the engineering design, laboratory testing and field trial of a solar powered water pumping system. The primary application is expected to be the supply of water for crop irrigation in developing countries or remote parts of Canada. As designed, the system can provide about 60 $m^3$ of water per day at a static head of 7 m based on a typical insolation of 18 $MJ/m^2$/day on a horizontal surface. The design process can easily be adapted to different flow and head regimes. The pump system consists of a 620 watt photovoltaic array, a DC motor and a single-stage, centrifugal pump.

The report deals mostly with the technical details of the system design, instrumentation, laboratory testing and field installation and operation. It is primarily intended for people interested in small-scale applications of photovoltaic power. The report and the pump system itself will, however, also be of interest to anyone involved in small-scale water supply and agriculture in developing countries or remote areas in Canada. While the report is not highly technical, the reader is assumed to have some knowledge of solar energy, photovoltaics, electronics and hydraulics.

The report is quite specific, describing a particular water pumping system. The report is not intended as a general treatment of water pumping, nor as an introduction to photovoltaics. Neither is it a user manual or instruction guide for the actual pumping system. Its findings should, however, be applicable to other, similar pump systems. Finally, the technology described in the report is proprietary to TPK International Inc. and the Crown, and therefore may not be used by any individual or organization in any way which would jeopardize the interests of the owners.

## ABSTRACT

In much of the world, ground or ditch water is raised a few meters to irrigate crops. For small fields in areas without grid power, photovoltaics can provide reliable and economical power to lift the water. Small, PV powered micro-irrigation pumping systems, consisting of a PV array directly coupled to a DC motor driving a centrifugal pump, are therefore being introduced into many developing countries. This report describes the construction, laboratory testing and field trial of a typical PV pump system designed to provide 60 $m^3$/day of water at a head of 7 m based on an insolation of 18 $MJ/m^2$/day.

The system was designed by selecting high-efficiency components which match each other as well as the application. A single-stage Leitch pump, a Reliance PM DC motor and 620 Wp of TPK PV modules were chosen. The components were tested in the laboratory and then integrated into a complete system. A PV powered data acquisition system was also developed to monitor the pump operation. Lab tests showed that the pump system operated as expected with a pump subsystem efficiency over 50% and a startup irradiance threshold around 325 $W/m^2$. The system operated around 70 volts, at a speed of 1900 rpm and flows up to 3.7 L/s, in agreement with the design calculations. Several problems with the sensors and data loggers had to be solved before dependable data were obtained.

The system was installed in a temporary field site and operated for four months during the summer of 1987. Performance data were collected and analysed regularly. Except for a few human errors, the pump system performed reliably, as did the data acquisition system after solving some startup problems. The daily results showed lower-than-expected pumped volumes, apparently caused by reduced pump efficiency. After the trial, the components were retested and grease, used as per the manufacturer's recommendation to install the pump seal on the shaft, was found on the pump seal where it was increasing the seal friction and reducing the efficiency. The flow meter was also found to be reading about 6% low. These two effects together fully account for the poorer than expected field results.

During the project, much was learned about testing, installation and operation of PV pump systems in the field. Further field trials and tests would be useful to further prepare the technology for marketing.

## EXECUTIVE SUMMARY

Throughout much of the world, irrigation is used to grow crops. In remote areas, however, it is often difficult to obtain power to lift the water onto the fields. In such situations, photovoltaics is emerging as a source of reliable and economical electric power. Thus, PV powered micro-irrigation pumping systems are now being installed in many developing countries. TPK has developed several such systems, but had not subjected them to extensive field trials. Therefore, the purpose of this project was to design, build and test a shallow-well PV pump system, subject it to a field trial and then evaluate the system and the trial results.

The system was required to pump 60 $m^3$/day at a static head of 7 m, based on a typical insolation of 18 $MJ/m^2$/day on a horizontal surface. The design involved selecting commercially available, high efficiency components which matched each other and the application for good performance over a wide range of operating conditions. The system consisted of a Canadian-made, Leitch single-stage centrifugal pump coupled to a Reliance 1/2 HP permanent magnet DC motor driven directly from a PV array having five series and four parallel TPK modules for a peak power of 620 watts. The nominal operating point was modelled using the component characteristics. Based on a typical irradiance of 800 $W/m^2$, the calculations predicted a current of 6.2 A at 71 V and a motor speed around 1980 rpm, giving a flow of 3.1 L/s at a total dynamic head of 7.5 m. The theoretical startup irradiance threshold was 325 $W/m^2$.

A data acquisition system was assembled to monitor the pump system. The solar irradiance, voltage, current, pump speed, discharge pressure, flow, and ambient and module temperatures were all sensed using a variety of transducers and customized conditioning circuitry. Two portable data loggers recorded the eight channels. For field use, the circuitry was powered by a 12 V battery charged from a separate PV module via a small shunt regulator.

Each of the pump system components was tested in the laboratory. The motor transforms voltage into speed and current into torque over a wide operating range, with a peak efficiency over 85%. The pump was tested over a range of speeds and flows, with the head and power being measured. The peak efficiency was 65%, some 8% less than the manufacturer's specifications (as expected), but quite good for a pump of this size. The PV array I-V curves were also measured and the results used to model the system performance over a typical day.

The complete pump system was tested in the laboratory and found to operate as expected. It was also tested outdoors during the winter, pumping an antifreeze solution around a closed loop. This test served to evaluate the system and debug the monitoring instrumentation, but otherwise was not very useful due to the effects of the antifreeze and low temperatures on the component operating characteristics.

The system was installed in the field in early May, 1987 and operated for four months. The site was on the Mississippi River in Almonte, Ontario and the pump provided water to an ornamental pool. The array was positioned facing true south at a 25° tilt in an open location with little shading. The plumbing was 2.6" (6.6 cm) ID pipe for minimal friction losses. The discharge height was periodically adjusted to maintain a 7 m static head as the river level dropped during the summer. The data loggers and their circuitry were placed in a rain-tight box on the array frame. Data were logged into a computer carried to the site at irregular intervals of one to ten days. Most of the time, only three channels (flow, voltage and sun) were logged to minimize travel and analysis time.

The flow and sunlight results were integrated on a daily basis to determine the insolation and pumped volume. Several problems were encountered due to human error, the data acquisition system, or the plumbing, which rendered some of the data incorrect or unreliable. No problems were attributed to the array, motor or pump. The recorded data were also analysed as parametric plots of flow, current and module temperature vs. solar irradiance, voltage vs. current, and so on. Most of these agreed with the predicted performance, but the flow and efficiency were lower than expected. Also, the dynamic pressure losses in the pipes seemed to be higher than calculated. The daily results showed an average volume of 51 $m^3$ at the design point, below the 60 $m^3$/day goal (although flows to a high of 90 $m^3$ on one day were realized).

After the trial, the components were retested in the lab to determine the cause(s) for the reduced output. The motor characteristics appeared unchanged. The brush wear indicated an extrapolated total brush life of 5,000 hours or about 26 months of field operation. At high flows, it was found that the flow meter had been reading 6% low. More serious, the peak pump efficiency had dropped to 50%. Upon inspection, it was found that grease used to install the pump seal on the pump shaft had gotten onto the seal face, thereby increasing its friction. After cleaning off the grease, the pump was retested and found to have its original efficiency once again. Hence, the design goals would have been met in the field if the seal had been clean.

Although the field results were disappointing in some ways, being marred by the grease on the pump seal, the field trial was very successful. A lot was learned about field installation and operation of PV pumping systems. Further improvements can be made to such systems to gain experience in real applications and to raise the public awareness of this promising technology.

## 1.0 INTRODUCTION

Perhaps the greatest and most widespread need currently facing mankind is the supply of water for crop irrigation and for human and livestock consumption. In developing countries in particular, the water supply problem is compounded by the lack of an electric power grid in many areas and by difficulties in obtaining dependable supplies of gasoline or diesel fuel to power water pumps. Both problems can be solved by providing reliable, on-site power generation to drive the pumps. In the past decade, photovoltaics has emerged as an effective approach for supplying power up to a few kilowatts in remote regions. Photovoltaics is already cost effective compared to diesel power in many applications, and is expected to become even more attractive in the future as module costs continue to fall [1,2].

Water pumping systems are projected to be one of the major markets for photovoltaic power over the next two decades [3,4]. For this reason, TPK has been active in developing and testing PV powered water pumping systems since 1981 [5,6,7]. The systems emerging from this program are comparable with those being supplied by other manufacturers and their performance has been confirmed by independent testing [8]. Hence, both shallow and deep well pump systems can now be confidently designed for a wide range of applications.

The design, construction and laboratory testing of PV pump systems is only the beginning. Before such systems can be successfully marketed they must be proven in actual field usage. Of the hundreds of pump systems installed in the field over the past decade, many are non-functional due to improper design, poor installation, unreliable components or lack of maintenance [9]. Hence, the need to pay proper attention to the details of design, construction, user manuals, installation and maintenance cannot be overstressed. The experience gained in the course of thorough field trials should eliminate most of these problems and ensure customer satisfaction.

The primary purpose, therefore, of this project was to perform a field trial on a typical photovoltaic pump system to gain experience in the installation and operation of such systems and to prove the design concepts and system components in actual usage. The pump system was specified to supply 60 $m^3$ of water at a static head of 7 m for a standard day with 18 $MJ/m^2$ of insolation on a horizontal surface. This specification represents the Type "B" system identified by the UNDP and Sir William Halcrow as a useful size for micro-irrigation applications [10]. Secondary objectives of the project were to design, construct and test the system in the laboratory, and to develop a PV powered data acquisition system

to monitor the pump system during its operation in the field. Finally, the field data were to be analysed and compared with the expected performance, and following the field trial, the system and its components were to be tested and re-evaluated.

The purpose of this final report is to describe the design and laboratory testing of the pump system as well as the data acquisition system, and to present and evaluate the field trial results. Section 2 of the report discusses the pump system design and component selection procedure. The data acquisition system is described in Section 3. Section 4 deals with the laboratory test methods and results while Section 5 presents the results of our initial outdoor testing. In Section 6, the pre-field trial results are analysed and evaluated. The field trial site and system installation are described in Section 7, while Section 8 presents and analyses the field trial results. In Section 9, the post-trial system evaluation is discussed. Section 10 presents conclusions and recommendations, and the report ends with references.

## 2.0 SYSTEM DESIGN

A block diagram of a typical shallow well photovoltaic water pumping system is given in Figure 1. The system is conceptually simple. The pump is driven by a motor which is powered by the PV array, which in turn derives its power from the instantaneous sunshine. The flow of water delivered at the operating head varies with the irradiance on the array. The design of this system consists of selecting a pump to deliver the water, matching it with a suitable motor, and determining how many PV modules are needed to drive it under the insolation available on-site. The components are sized by working backward along the energy conversion chain, taking into account the losses at each stage [6].

The design begins with a typical operating point derived from the system specifications. While the system parameters change throughout the day, an "average" or typical operating point can be selected. This usually corresponds to an irradiance mid way between the startup threshold (typically 300 to 500 $W/m^2$) and the peak irradiance of 1000 $W/m^2$. A value of 800 $W/m^2$ is a good choice for sunny locations. At this irradiance, the daily insolation of 18 $MJ/m^2$ is obtained in 6.25 hours of operation. This can be reduced to 6.0 to discount the sub-threshold sunshine which is wasted. Thus, to accumulate 60 $m^3$ of water during this period, the typical flow will be 10 $m^3/hr$ or 2.8 L/s (44 usgpm). This flow must be delivered at the static head of seven meters, plus any dynamic head losses (estimated at 10% of the static head), giving a total of, approximately 7.5 m.

A pump is now selected to match the flow and head. For this application, a single stage, direct-coupled centrifugal pump is best [6]. Such pumps are inexpensive, widely available, simple, reliable and efficient. No transmission is required between pump and motor, and the locus of operating points for the pump-motor subsystem matches the PV array fairly well without the use of electronic load matching circuitry (ie. a maximum power tracker [11]). In selecting a pump from manufacturers' data, the similarity rules for centrifugal pumps can be applied to determine how the pump will operate at different shaft speeds. For a given pump, the total head (H) is proportional to the square of the shaft speed (s), while the flow (Q) is directly proportional to the speed [12,13]. In PV pump systems, it is a good idea to select a large pump and operate it at a relatively slow speed (around 1800 RPM for example) to take advantage of the higher efficiency of larger centrifugal pumps [14].

There are several manufacturers who make suitable, high efficiency centrifugal pumps. Most are very similar in construction, having closed bronze impellers, cast-iron volute casings and carbon ceramic seals. For this system, the nominal operating parameters were best matched by a Leitch 1 1/2 CAC pump with a 5.0" (13 cm) diameter impeller. The H vs Q curves supplied by the manufacturer for this pump are described in Section 4. This Canadian-made pump has a 2" inlet and a 1.5" discharge, both threaded for NPT couplings. With a 5" impeller, this pump should operate at peak efficiency at the design head and flow when turning at about 1974 RPM (calculated from H-Q curves for 1750 RPM using the similarity rules). From previous experience [6], the stated efficiency (over 70%) is never achieved in practice - the best that can be hoped for is a value 5 to 6% lower. Therefore, the expected peak (nominal design point) efficiency for this pump is about 65%. This is considered quite good for this size of pump [14]. To improve the efficiency by reducing friction, the inside of the pump casing was smoothed down and filled with an epoxy resin.

The hydraulic power delivered by the pump is the product of flow, head, density of water and the acceleration of gravity (see Figure 1). At the design point, the value is 206 watts (2.8L/s X 7.5m X 1.0kg/L X 9.8m/s$^2$). The mechanical shaft power needed to drive the pump is therefore, $P_{hyd}$ divided by the pump efficiency (65%), giving 317 watts. Thus, a 1/2 HP motor should be sufficient. For PV pump systems at present, permanent-magnet, brush-type DC motors are still the best choice [6,9]. They are reliable, robust, relatively inexpensive, simple to use and are the most efficient of all motors below about 2 HP. A TENV (totally enclosed, non-ventilated) type is best for outdoor use. Again, several manufacturers supply suitable motors. The motor is selected from a limited number of models on the basis of power, shaft speed and nominal voltage.

The Reliance model T56H 3203N-VM was selected for the system. It is specified to operate at 90 V and 2500 RPM. It has an EC56C frame for direct mounting to the pump. On the basis of its specifications, it should have an efficiency of about 80%. In a PM DC motor, the shaft speed is directly proportional to the voltage. Thus, the motor should turn at 1974 RPM when operated under load at about 71 volts. The electric power is calculated by dividing the shaft power by the motor efficiency, giving 396 watts. Thus the nominal operating current should be about 5.6 A.

The characteristics of the PV modules available for use in this system are listed in Table I [7]. The modules are mounted on a portable support structure with an adjustable tilt

(0 to 45°. Each has a peak power at 25°C and 1000 W/m$^2$ of about 31 W at a voltage around 16V. Under the design condition of 800 W/m$^2$ sunshine and an operating temperature of 50°C, each module can be expected to produce about 1.55 A at 14.2 V. Thus, for 71 volts, five series modules (71 V) are required and for 5.6 A, four parallel modules (6.2 A) are needed, giving twenty modules in all for a peak power rating of 620 Wp at about 80 V. This concludes the initial system design.

With the major system components selected, the design calculation can be reversed to predict the actual system performance. The array power available at 800 W/m$^2$ and 50 °C typical cell temperature is 6.2 A X 71 V = 440 watts. With the system voltage so close to the maximum power point, essentially all of the power will be delivered to the motor. The shaft power will therefore be 80% of this, or 352 W and the hydraulic power will be 65% of that result, or 228 watts. At a total head of 7.5 m, this represents a flow of 3.1 L/s which, over 5 to 6 hours of daily operation provides a total pumped volume of 56 to 67 cubic meters. This, of course, is only a rough estimate as the pump does not operate at one point all day long and resistive losses in the power cable have been ignored.

There are other important system performance parameters which can be estimated. Assuming there is no shaft coupling loss, the wire-to-water efficiency is simply the product of the pump and motor efficiencies: 80% X 65% = 52%. The system startup threshold (the irradiance level at which the pump starts delivering water) cannot be predicted with any accuracy since the pump efficiency is zero at no flow and the manufacturer gives no information on power required at cutoff (static head, no flow). This parameter should ideally be as low as possible since any solar irradiance below this level is wasted.

At the other end of the operating range, the peak flow at 1000 W/m$^2$ sunlight can be estimated. The peak array power at 50°C should be about 550 watts at a voltage around 70 to 73 volts. If the motor operates at a somewhat higher voltage (say 75 volts or so), then the electrical power to the motor should be just slightly less since the array is operating away from its maximum power point - say 96% or 528 W. The shaft power will then be 422 W and the hydraulic power about 275 W, giving a peak flow of 3.7 L/s (59 usgpm). The current will be about 7.0 A. These peak values are useful in sizing the power cable and system plumbing. The wire gauge in the cable is chosen, depending on the distance between the array and the motor, to minimize the resistive losses. The pipe diameter is chosen to minimize the head losses caused by friction [12]. For this system, a 2" I.D. discharge pipe was initially selected - the same size as the pump inlet.

## 3.0 DATA ACQUISITION SYSTEM

Part of the project was to monitor the pump system operation on a continuous basis and to develop a PV powered data acquisition system to serve this purpose. In such a system, the operating parameters are sensed by transducers attached to the pump and array. Their electrical signals are conditioned and sent to a data logger which regularly measures and records the signals. The stored data are periodically read back for plotting and analysis. The parameters to be monitored and their expected operating ranges are as follows:

- global solar irradiance on the array (0 to 1000 $W/m^2$)
- array voltage (0 to 100 volts)
- array (or motor) current (0 to 10 amperes)
- ambient temperature (0 to 40°C expected)
- module temperature (0 to 30°C above ambient)
- motor shaft speed (0 to 2500 RPM)
- pump discharge pressure (0 to 10 m $H_2O$ head)
- pump flow (0 to 5 L/s)

The heart of the data acquisition system is the data logger. After considering several commercially available models, the Rustrak Ranger, supplied by Gultan Industries was selected. This is a small, inexpensive, battery powered logger which can be adapted to a wide range of signal types and recording periods. The unit can record up to four channels. Thus two units were obtained for the eight signals listed above. The inputs are 0 to 2 V analog or 0 to 20 kHz pulse rate (counting) and can be programmed for different types of signals. The analog signals are sampled every 650 ms as 12 bit digital words. The data are played back to an IBM PC 9 or compatible) computer via a serial cable. The units are supplied with plotting and analysis software which, among other functions, allows the user to display or integrate the data on a daily basis.

This data logger can store about 400 data points per channel in its memory. The microprocessor monitors the data being read and stores it in a flexible format. The time between stored values is adjusted to fill the memory by the end of the programmed recording period. During each logging interval (about four minutes for a 24 hour recording session), the unit keeps track of the maximum, minimum and average values of the signal and stores these rather that actual signal values in its memory. If the signal is constant, the logging interval will be longer than if the signal varies a lot. The unit also trades off memory among the four channels, allocating more to those signals which change more frequently. Finally, as the memory is filled, the microprocessor may rearrange the stored data,

packing some of it into less space to conserve memory until the end of the recording session. Thus, on playback, some of the record may be quite detailed while other channels or time periods may be rather sparse. The analysis software interprets the stored data and then plots it, interpolating through the logging interval as either a straight line or a parabola. This effect is described further in section 5.

In what follows, the transducers and their associated signal conditioning circuitry are described. The schematic diagram for the circuit is given in Figure 2. The transducers and pump system components are along the left edge of the figure and the data loggers are shown on the right. The signal conditioning electronics, assembled on a circuit board, occupies the centre of the diagram. To simplify the power supply design, the signal conditioning is done using single-supply operational amplifiers which can operate with inputs down to zero volts.

Power for the data acquisition system is provided by a single TPK SW1803 PV module. This supplies up to 1.2 A to charge a 12 V gelled-electrolyte battery via a small shunt regulator. The module and battery are sized to provide continuous power to the loggers and the electronics. Each logger has a 4 V NiCd battery which is trickle charged from the main battery. The negative of the battery is grounded to earth and also serves as the circuit ground on the PC board. All of the signal cable shields are grounded. The battery, data loggers and electronics are all enclosed in a rain-tight metal box for field usage.

The flow meter is an Omega model FP-5300 paddle wheel type. As the paddle turns, it induces an AC voltage in a sensing coil. The amplitude and frequency are both proportional to the flow rate. The input diode (see Figure 2) shorts out the negative half cycles while the LM324 operational amplifier increases the signal amplitude. The high gain and the subsequent CMOS inverting stages ensure that the output signal is a constant-amplitude square wave with the same frequency as the flow sensor. This signal is then attenuated to the 2 V level needed for the data logger. Pin 2 of the logger is the counting input. Pin 3 (ground) is common to all four channels. The analog input on pin 4 of channel X1 is grounded to prevent noise problems at the high impedance inputs of the logger.

Channels X2 and X3 are respectively the array voltage and current signals. The high array voltage is attenuated and buffered by a unity-gain amplifier before going to the logger input. The two series LED's serve to clamp the voltage at about 2.5 V in the event of a circuit fault or transient (the data loggers can be damaged by input voltages above 3 V). LED's were

used as they have better switching characteristics than low voltage zener diodes. The array current is sensed by a 5 milliohm shunt. This millivolt signal goes through a low-pass filter to remove spurious noise and is then amplified before reaching the input of channel X3, which is protected by another voltage clamp. The counting inputs of the analog channels are grounded.

The ambient temperature is measured by an AD590 temperature sensor suspended in the shade behind the PV array. This sensor has an output of 1 microamp per degree Kelvin. The precision input resistor converts this to a voltage signal which is buffered and passed to the protected analog input of channel X4. An identical circuit senses the module temperature for channel Y4 of the second data logger. In this case, the sensor is fastened to the back of one of the modules, behind a solar cell and thermally insulated from the surrounding air.

Rotation of the motor shaft is sensed by a reflective LED-phototransistor pair mounted on the pump casing. The coupling between pump and motor is painted half black and half white. As the shaft turns, a signal is generated at the emitter of the phototransistor - one cycle per shaft revolution. This signal is squared up through a pair of inverters, attenuated and passed to the counting input of channel Y1.

The system operating pressure is sensed at a small tap ten pipe diameters from the pump outlet by an Omega model PX105-050G5V pressure transducer with a range of 0 to 50 psig. This transducer is driven by a regulated 8 V supply and has an offset of about 1 volt at zero pressure. The pressure signal is attenuated, buffered and passed to the voltage-clamped analog input line of channel Y2. Pressure readings have to be adjusted for the electrical offset as well as the static head between the inlet water level and the transducer.

Initially, the instantaneous irradiance was measured using a Hollis pyranometer mounted above and in the same plane as the array. The first unit failed after a few days outdoors during initial setup of the system. Its output dropped to a low value. The second, identical unit appeared to function correctly at first. After a few months outdoors, however (over the winter), its readings became suspect when the array output appeared to become unstable. Failure was confirmed by comparing the unit against an Eppley pyranometer (courtesy of Jacques Domey, Division of Electrical Engineering, National Research Council of Canada). Thus, the Hollis pyranometers (both several years old) were retired and replaced by a small calibrated solar cell mounted on an aluminium heatsink. The calibration was regularly checked against that of the Eppley pyranometer which

is traceable to independent international standards. The sun sensor circuit was modified for the standard solar cell and is as shown in Figure 2. The cell current is converted to a voltage by a one ohm resistor, buffered, amplified and conducted to the analog input of data logger channel Y3.

Once the data acquisition system had been constructed, installed, tested and debugged, all eight channels were calibrated and checked for zero offset readings (taken at night) and nonlinearities. The results are presented in Table II. The estimated uncertainity for each of the signals is also given in the table. The flowmeter was calibrated in the lab by weighing a timed volume of water pumped during steady state system operation. It was found to be slightly non-linear with a conversion constant between 5.8 and 6.9 LPM/Hz (compared to 6.77 specified by manufacturer) over the range of flows for this application. At low flows (less than 35 Lpm or 9 usgpm), the flow meter readings became erratic, and the paddle wheel did not turn below 20 Lpm.

The array voltage and current were calibrated using digital multimeters accurate to about 1%. There was some offset in the current reading because of the low signal level from the shunt and the input offset voltage of the LM324 amplifiers. This appeared to be constant, however, and in any case was recorded every night by the data logger. The two temperature sensors were calibrated at night using a thermometer. Although their circuitry was identical, the two had slightly different conversion constants, because of resistor and sensor tolerances.

The shaft speed measurement should be as accurate as the crystal controlled time base of the data loggers. In the field, the reflective sensor had to be shaded from direct sunlight to avoid problems. The pressure reading is not quite as simple. For the transducer selected, the dynamic range is only 0.4 volts or so, comparable to the zero offset. Also, for hydraulic reasons, the pressure tap must be at least ten pipe diameters from the pump discharge to ensure correct readings [13]. Thus, the measurements must be corrected for static head and dynamic friction losses. Fortunately, the transducer was linear. Its calibration was done using a large bourdon gauge which had previously been checked [6].

As mentioned above, the sun sensor was calibrated against a good standard. It was linear over the range of interest for this project. There was some offset in the signal to the data logger. The results varied slightly with ambient temperature and with the position of the sun in the sky - hence the estimated 2% uncertainty relative to the calibration standard.

## 4.0 LABORATORY TESTING OF SYSTEM COMPONENTS

Prior to placing the pump system in the field, laboratory testing of the major components was performed to characterize their individual performances. The results of these tests were used to compare with manufacturers' claims, to validate the system design procedure and to provide data for predicting system performance in the field. The results also serve as a baseline for determining the effects (if any) of the field trial on the components.

The DC motor was tested using a technique previously developed at TPK [6]. In this test, the motor shaft was coupled to that of a second, similar permanent magnet motor which was driven as a generator. The test motor was powered by a variable DC supply and the generator load was a rheostat. The currents and voltages of the motor and generator were measured under steady state operartion for a wide range of voltages and for loads from zero torque (no load) to zero speed (stall). The shaft speed was measured at the same time. By calculating the known losses in the motor and generator, the shaft power at each operating point (and thus, the torque and efficiency) could be calculated quite accurately. The results were then plotted in graphical form.

The test results for the Reliance motor are presented in Figure 3. In this figure, lines of constant speed, torque and efficiency are plotted on the current vs voltage plane. As in any PM DC motor, speed is proportional to voltage and torque is proportional to current. The slope in the constant speed lines represents the DC series resistance of the motor. The zero torque (no load) curve represents the power required to overcome brush friction, windage and other speed dependent losses in the motor. No testing was done below 30 V. The motor was tested at its full-load operating temperature (about 10$^{o}$C above ambient). The nominal (rated) operating point and the design point for the pump system are both shown on the figure, but the motor can be operated anywhere on the plane. The efficiency was higher than expected and very good for a motor of this size: 85 to 86%.

The laboratory setup used to test the pump is depicted in Figure 4. In this test, water was circulated around a closed loop from a holding tank. The pump inlet was flooded to avoid priming problems. The 1.5" discharge expanded to a 2" diameter pipe to reduce friction loss. The pressure was controlled manually with a gate valve and read on a bourbon gauge as well as the pressure transducer. The open air discharge flow was collected and returned to the tank by a "U" tube which contained the flow meter. The pump was driven by the previously

characterized motor from a variable DC power supply. The shaft speed, pressure and flow signals were read off the data logger displays.

For testing, the pump was operated at a constant shaft speed by adjusting the motor voltage. The gate valve was then adjusted to change the total dynamic head from a minimum value of about three meters (fully open) to cutoff (fully closed). The system was allowed to stabilize for a minute or so and readings of voltage, current, speed, pressure and flow recorded. Data sets were taken for several fixed values of shaft speed. Following the test, the data were analysed to find the total dynamic head and efficiency at each operating point. From the voltage, current and speed, the shaft power was determined using Figure 3. The total head was found by adding the measured pressure, the static pressure from the tank water level to the pressure tap, and the friction losses in the inlet and discharge plumbing [12,13].

The results for the Leitch pump are plotted as H vs Q curves in Figure 5. A single curve (1800 RPM "expected"), calculated from the manufacturer's data sheet, is included for comparison. On the "expected" curve, the efficiencies have been reduced by 6%. This appears to be a good assumption at low flows, even though the expected and actual curves have different hydraulic heads. At higher flow rates, the efficiency is somewhat lower-than-expected and the pump acts like a smaller pump, with its peak efficiency occuring at a lower than expected flow. This may be due to the epoxy used to smooth out the pump casing. The efficiency is still quite good, however.

The other curve shown in Figure 5 is an assumed load line or operating curve for the as-designed pump system. This curve starts on the left at the static head and zero flow (cutoff) and curves upwards toward the right in a shallow parabola which represents the additional friction losses in the plumbing. The nominal operating point at the design flow is indicated on this curve. The position of this curve and point, close to the area of maximum efficiency, confirms that the pump is well suited to this application. The system should operate very efficiently over a broad range of sunlight levels.

The third major component in the system is the PV array. The current vs voltage curve for the array was measured on a clear day in January, with the array clean and dry, and the module temperature around 27°C. The measurements included the effect of resistance in the power cable. Since the pyranometer readings at that time were later found to be unreliable, the short circuit current under full sunlight was measured later, after a reliable sun sensor had been obtained. The temperature and light intensity effects on the solar cells had also been

previously measured. Thus, it was possible to correct the I-V measurements to standard conditions of 1000W/$m^2$ and 25°C. The results, along with the expected array parameters from Table I, are tabulated as follows:

| array parameter | expected | measured |
|---|---|---|
| short circuit current | 9.0 A | 8.65 A |
| open circuit voltage | 102 V | 102.3 V |
| maximum output power | 620 W | 590 W |
| maximum power voltage | 80 V | 79.5 V |
| curve fill factor | 66 % | 66.5 % |

Note that the measured peak power was less than the expected value for the array. Since the open circuit voltage and fill factor were as expected, the difference (about 4%) was entirely in the short circuit current. This is most likely attributed to the uncertainty in sunlight measurement rather than to an actual change in module characteristics.

The I-V curves shown in Figure 6 were constructed on the basis of the measured curve and the known temperature coefficients of voltage and current for this type of solar cell. The module temperatures were estimated for an ambient temperature of 25°C using the module heating data presented in Section 6. For each curve, the maximum power point was found, and the dashed curve is the locus of these points. The I-V load line included in the figure for the pump subsystem was taken from the simulated field data described below. Its significance will be discussed later.

With each component characterized, the pump subsystem, PV array (set up outdoors) and data acquisition system were connected togther and allowed to operate for several days. Since the static head in the laboratory was only about three meters, the gate valve was set at an arbitrary point and the head allowed to vary with flow during most of the daily operation. Thus, the data collected are not particularly useful. This indoor trial did serve, however, to check the memory limits of the data logger and the operating limits of the pump system. For one clear afternoon (March 13, 1987), the gate valve was periodically adjusted to maintain the head vs flow load line shown in Figure 5. The idea was to simulate a half day of field operation to obtain data for comparison with theory. The ambient temperature at the array was 5 to 8°C during this test and the simulated static head was actually 6.9 m so the design conditions (25°C and 7 m head) were not exactly met. However, the results should allow for qualitative comparison with theory.

Some of the representative data points are presented in Table III. The data were recorded from the data logger displays and then converted to appropriate units using the conversions given in Table II. These data are used in Section 6 for comparison with theory. Solar noon on that day occured at about 12:10 but the peak in the array output was around 12:35. This indicates that the array was probably oriented a few degrees west of south. The array was tilted at about 45° during these tests. Testing stopped when the flow fell to zero. This occured at an irradiance of about 305 $W/m^2$, the startup threshold for the system.

The actual operating point at 800 $W/m^2$ can be estimated from these data by interpolation. The results are compared with the nominal operating point design calculations from section 2 in the following table:

| operating parameter | design | actual | units |
|---|---|---|---|
| time of day | N/A | 14:54 | EST |
| solar irradiance | 800 | 800 | $W/m^2$ |
| ambient temperature | 25 | ~7 | °C |
| total head | 7.5 | 7.25 | m |
| flow rate | 3.1 | 3.25 | L/s |
| shaft speed | ~1980 | 1992 | RPM |
| array voltage | ~71 | 71.9 | V |
| array current | 6.2 | 6.21 | A |
| array power | 440 | 446 | W |
| module temperature | 50 | 28.6 | °C |

Although the actual ambient temperature and head, as well as the pump characteristics are quite different from those assumed in the design, the operating point is very close to the expected parameters. The voltage, flow, current and shaft speed in particular are as close as can reasonably be expected. Hence, the design process and calculations appear to be valid.

## 5.0 OUTDOOR TESTING

When the pump system was first assembled, it was set up outdoors behind TPK's plant in City of Nepean for testing along with the data acquisition system. The setup was similar to that shown in Figure 3 except that both the discharge and return pipes were extended to produce a true static head of seven meters. Since the tests were performed in late November and early December, antifreeze was added to the water to prevent freezing (which would have damaged the pump and plumbing). Ethylene-glycol based automotive antifreeze was used at a volume concentration of about 30%, effective to about -18°C. This was necessary as the ambient temperature dipped to about -20°C one night.

The cold temperature caused several problems. The offset voltage on some of the sensors used to monitor the operation changed slightly. On several occasions snow had to be swept off the array, or the array was covered in partially melted ice. The low temperature, coupled with ice crystals and the possibility of reflections also affected the sunlight readings from the pyranometer. Snow would also drift around the pump and motor even though they were loosely covered with plastic. Finally, when the pump was operating, there was some loss of fluid due to splashing at the top end or in the barrel at the return end. Thus, the level had to be topped up every second day or so with a combination of water, antifreeze and whatever snow had fallen.

The pump system was operational outdoors for a total of 23 days summarized in Table IV. During this period, tha data acquisition system was being set up, tested, characterized and debugged. Some recording was done on 20 days and on 9 of those, the data acquisition was operating properly so that complete records were obtained. The remainder of the time, either one or another sensor circuit was being worked on. Most of the problems encountered involved electrical or optical noise, or a sensor signal problem. The first pyranometer malfunctioned at this time. Table IV also includes the integrated flow (pumped volume) and sunlight (insolation) for each day's recording period. Outdoor testing was stopped in mid December when the liquid level dropped below the pump inlet and the pump started to draw air and lost its prime.

The best data were obtained on December 8. All eight data channels were functioning correctly and the day was mostly clear. Computer plots of all eight channels are presented in Figure 7. The channels are labelled with their signal scale (in hertz or volts as seen by the data logger), time of day (eastern standard time) and other appropriate information. These data

were taken before some of the channels had been properly calibrated. Thus, the conversion coefficients shown in some cases differ from those given in Section 3.

With reference to the flow meter and irradiance data plotted in the first two graphs of Figure 7, non-zero flow is first recorded at about 9:18 AM, at an irradiance of 595 $W/m^2$. The system had actually started pumping earlier, but the flow meter did not turn until the flow reached some minimum point. Notice that the flow data are much noisier than the solar irradiance curve. The pump flow is inherently turbulent and thus produces a noisy signal. In addition, air entrapment in the return pipe caused an irregular "surging" in the return flow which changed with varying flow rates. The late afternoon was marred by cloudy periods which caused the flow to stop and start rapidly. Just before sunset, the shadow of the building cut off direct radiation from the sun.

The array voltage and current data appeared to be well behaved. The current correlates very well with the irradiance. The sharp bend in the voltage graph indicates where the system starts pumping: about 8:53 AM, at an irradiance of about 490 $W/m^2$. The two temperature plots in figure 7 can be compared to determine the module heating during the day. Both plots are very noisy, indicating the effects of random gusts of wind. After sunset, the array, exposed to a clear sky, cools down faster than the "ambient" temperature in the sheltered area behind the array.

The motor speed data correlate well with the voltage plot (as they should), beginning when the data loggers were started at about 8:23 AM. The head or pressure curve shows an even sharper bend when the static head was first achieved. From these data, the static head appeared to be 7.32 m rather than 7.0 m. This was because the specific gravity of the antifreeze solution was 1.042 rather than 1.00 for pure water.

For numerical analysis, the data stored from the loggers were printed out. A sample of the data from two of the December 8 records is presented in Table V. This shows the format in which the data are stored in the logger for display and analysis. Some of these data were analysed manually. The results are not particularly useful however, because of the low temperature, higher fluid density, pyranometer uncertainty and uncalibrated flow meter. In addition, at $-20^{\circ}C$, the antifreeze solution has a high viscosity [15] and this has a significant but uncertain effect on the pump performance [13]. After correcting for density and flowmeter calibration, the peak subsystem efficiency was calculated to be about 54% - very close to the expected value. Thus, the data are reasonably accurate

in spite of the uncertainties. In any case, the outdoor testing did serve the purpose of demonstrating the operation of both the pump system and the data acquisition hardware over an extended period under "real" (even extreme) conditions.

Part of the purpose of the outdoor testing was to determine the capabilities of the data loggers. During the test period, data were recorded over different time periods, ranging from a few hours to about eight days. Over a single day or eight hour period as shown in Figure 7, the data are quite detailed, the typical recording interval being about 2 minutes. Over a longer period, however, as discussed in Section 3, the data are much more sparse. Figure 8 illustrates this effect. The loggers were programmed for 7 days of storage and stopped after 5 1/2 days of recording.

Some of the channels (ie. X1, X4, Y1, Y2 and Y4) in Figure 8 appear to be complete, showing detailed daily peaks. In the record for channel X3 (array current), however, the data starts off properly, and then becomes sparse, the night time flats being replaced by broad parabolas. Channels X2 and Y3 illustrate extreme cases of this effect. In these plots, two or more days are represented by a single parabola, rendering the data useless. What happened was that, in an effort to conserve its limited memory, the logger has compacted the data in one or more channels. There is no way to prioritize the channels to force compaction in a less important channel.

## 6.0 ANALYSIS AND EVALUATION

Once accurate performance characteristics had been obtained for each of the three major components, the operation of the entire system was simulated to predict its daily performance in the field. A graphical approach to the modelling was used and the operating parameters were calculated under different conditions, starting at the pump discharge and working backward along the energy conversion chain (Figure 1) to the array and solar irradiance. The numerical results of this form of modelling are presented in Table VI.

The simulation began with a hydraulic load line superimposed on the pump H-Q curves as shown in Figure 5. This load line models the static head (7m) plus dynamic friction losses in the discharge plumbing (proportional to the square of the flow). Points along this curve, from cutoff to peak flow, were selected and the flow, total dynamic head, pump efficiency and shaft speed read off the axes of the graph or estimated by interpolation. Thus, the first four rows of Table VI were filled in. The hydraulic power was calculated from the flow and head. Dividing this by the pump efficiency yielded the mechanical or shaft power at each operating point. The shaft power at cutoff was estimated by extrapolating the previous values to zero flow. Finally, the torque was found from the shaft power and speed.

Attention now shifts to the motor characteristics plotted in Figure 3. The speed vs torque points were located by interpolating between the curves to yield the electrical load line for the system. The voltage and current values were read off the axes of the graph, and the motor efficiency estimated from the curves. The electric power was determined from the voltage - current product at each point. The wire-to-water or subsystem efficiency was then determined as the product of the pump and motor efficiencies or as the ratio of hydraulic to electric powers. Any voltage drop in the power cable from the array could have been added to the voltage readings at this time to model the cable resistance.

After transferring the I-V load line to the array characteristics as shown in Figure 6, the irradiance required at each operating point was estimated by interpolation. The ambient temperature and module heating effects were included in the array I-V curves as discussed in Section 4. From Figure 6, the threshold irradiance appears to be around 325 $W/m^2$. This compares with the 305 $W/m^2$ threshold from the March 13 data at a 6.9 m head (Table III). The December 8 threshold value of 490 $W/m^2$ was much higher because of the denser and more viscous fluid as well as the effects of low temperature on the array and other components. Note that this model does not simulate the

sub-threshold operation of the system. The sub-threshold load lines in Figures 3 and 6 were measured and have been added to the figures for completeness.

The calculated operating points from Table VI can be graphed as parametric plots. Figure 9 presents plots of voltage, flow and subsystem efficiency (the most interesting parameters) versus irradiance. The March 13 data from Table III are also plotted for comparison. Generally, there is agreement between the two. Most of the discrepancies were caused by the difference in static head and ambient temperature, and by the cable resistance (the modelled curves were based on motor voltage while the data logger measured array voltage). Note that the subsystem efficiency is high when the irradiance is above 500 $W/m^2$, especially at the 800 $W/m^2$ design point.

The final step in the modelling was to simulate a day's operation. This was done as shown in Figure 10. Only half a day is shown since the afternoon should mirror the morning. The irradiance curve was adapted from the March 13 data (Table III) as a "standard" solar day; perfectly clear, 12 hours of sunlight and a peak of 1000 $W/m^2$. At each time of day, the irradiance was determined and the corresponding value for the parameter of interest found from Figure 9. In this model, the pump startup threshold occurs around 7:38 AM, and operation at the 800 $W/m^2$ design point is indeed typical. The subsystem efficiency rises quickly above 50% and stays there for more than seven hours. The peak flow reaches 3.8 L/s - in agreement with the design calculation.

The daily pumped volume was found by integrating the half-day flow curve and multiplying by two. A value of 88.4 $m^3$ resulted. The corresponding integral for the irradiance yielded an insolation of 26.0 $MJ/m^2$. In contrast, the design value was 18 $MJ/m^2$ on a horizontal surface. This was meant to be an "average" day. To simulate this insolation, the "standard" irradiance given in Figure 10 could have been scaled to reduce the insolation to this level, but that would not have made it an "average" day since the peak sun would have been reduced to only 700 $W/m^2$. The increase in insolation from a horizontal surface to the tilted array (depending on the latitude) further complicates the matter. In reality, a true "average" day is a combination of clear and cloudy days during different parts of the year, and perhaps could be better modelled as the "standard" day of Figure 10 with a few cloudy periods. The pumped volume would then be proportional to the insolation, as a first approximation. If this is the case, an 18 $MJ/m^2$ day should produce a total pumped volume around 61 $m^3$, just over the design value of 60 $m^3$.

One final parametric plot is presented in Figure 11 where module temperature rise is plotted against irradiance on the module surface. The data points are from the March 13 and December 8 data (module temperature minus ambient). The curves are representative of heat transfer by convection and radiation (in still air with light winds) [16]. (Values from the lower curve were used to set the module temperature shown in Figure 6.) There is a lot of scatter in the measured data,indicating that gusts of wind and thermal-mass effects in the array play important roles. Fortunately, the module temperature has only second order effects on the system operation so that the scatter in Figure 11 would not effect the other data significantly.

After the outdoor testing, the pump subsystem was disassembled and its component parts examined. The exposed metal inside the pump casing had begun to rust as is normal for cast iron. The epoxy filler used to smooth out the casing surface appeared to be in good condition, but the paint sprayed over it had started to blister and lift off. This should not have affected the pump performance. The graphite-ceramic seal was in good condition, as was the rest of the pump. The motor appeared as-new, with no rusting, in spite of being frozen and dusted with snow regularly. The bearings were smooth, and the no-load current the same as initially. Finally, the brushes were removed, examined and measured. They were, of course, slightly worn, but not yet enough for an estimate of their expected life.

In solar pumping systems, where the array is connected directly to the motor, there is always the question whether or not some form of maximum power tracking should be used to obtain a better match between the source and load [6,11]. The operation of a maximum power tracker (MPT) can best be understood with reference to Figure 6, where the electrical charactersitics of the system are plotted. An MPT would ensure that the array always operates at its maximum power point; ie. along the vertical dashed curve [11]. The same MPT, however, also has internal losses, characterized by a tracking efficiency; the ratio of load or output power to maximum array power. This efficiency is typically 90 to 95% so that for every 100Wp of available power, the load receives 90 to 95 watts [11]. In Figure 6, the actual load line for the pump subsystem is very close to the locus of maximum power points. In fact, the ratio of load power to available power is always above 94% while the system is pumping. Thus, in this case, an MPT is useless - the source and load are well matched without one.

An MPT adds cost and complexity to the system and may affect its reliability. Therefore, use of an MPT is justified only when the source and load would otherwise be poorly matched,

such as with a positive-displacement type pump [6]. In the system characterized by Figure 6, this could happen if the ambient temperature changed by more than 25°C, or if the static head changed by more than 35%. (With given components, these are the only conditions which will shift the source or load curves by 10 volts which would be needed to consider an MPT.) Since none of these extremes are anticipated for the present system, the option of using any type of MPT can confidently be ruled out.

From the results obtained in the foregoing tests, the type "B" pump system appears to be well designed. Both the pump and motor are efficient and well suited for this system. The laboratory testing showed that the pump has characteristics significantly different from those specified by the manufacturer: a lower efficiency (as expected) and significantly different head vs. flow curves. In spite of these variances, the simple design calculations done in Section 2 yielded a good estimate of the system performance. From the initial results, the design goals appear to have been met. The system should be able to pump 60 $m^3$ at a 7 m head during a "typical" 18 $MJ/m^2$ day. Moreover, the modelled parametric plots in Figure 10 agree reasonably well with the actual measured data. Thus, the system operated as it should have and is well understood.

Most of the problems encountered were associated with the data acquisition system. These involved the primary transducers (eg. pyranometer instability and flow meter non-linearity), the wiring (noise and proper grounding), and the signal conditioning circuitry (offset voltages and pulse-shaping electronics). All of the problems were solved, however, and the data acquisition system provided reliable information on the pump system performance.

## 7.0 FIELD INSTALLATION

A site was selected for the field trial about 50 km west of Ottawa in Almonte, Ontario, on the Mississippi river. The private lot (courtesy of Anne Campbell, an Almonte resident) had a steep slope down to the river to provide the 7 m head and was open on the south side for the PV array. Prior to installation, the site was visited to determine the best locations for the array and pump as well as the lengths of cables and pipes required.

The system was installed May 1-7, 1987. The array was positioned on the south side of the house, facing true south, inclined at a $25^{o}$ angle for summer use. The location was selected for minimal shading during the summer months. The only shading came from a hydro wire and a small tree in the late afternoon in August. The trailer-mounted array was first positioned and then the wheels were removed. The trailer frame was then anchored in place and tied down against winds with wire guys. A photo of the installed array is shown in Figure 12.

The pump and motor were installed on the river bank, behind some bushes, at the base of a rock face about 3 m high. They were mounted on a wooden base plate with a loose-fitting sheet metal cover (see photo in Figure 12). This location was selected to minimize the horizontal run of the pipe. To further reduce friction losses, large diameter (2.6 inch, 6.6 cm) PVC and smooth steel pipes were used for most of the plumbing. Above the rock face, the discharge pipe continued up the slope to a tree where it was tied in place. The pumped water splashed into an ornamental pool and from there flowed back down to the river. The discharge included a section of flexible pipe to make head adjustments easy. The 25 ft. long (7.6 m) suction pipe angled down into the river at $20^{o}$. It ended at a $45^{o}$ angle with a rubber-flapper type footvalve and a basket strainer made from coarse galvanized steel screen.

Initially, most of the suction pipe was submerged and the discharge was more than a metre above the pool. As the river level dropped during the summer, the discharge was moved down the tree to maintain a constant 7 m static head. The initial head was measured carefully. The pipes, elbows, footvalve and other flow restrictions were analysed to estimate the total dynamic head loss due to friction [12]. This loss varies as the square of the flow and was 56 cm of head at 3.0 L/s flow. The calculated result was more than expected, even with the relatively short pipe lengths and large diameters selected.

Since the PV array was about 140 ft (43 m) from the pump, a #6 AWG power cable was used to minimized the voltage drop due to series resistance. The resistance was about 0.12 ohms, giving a peak voltage drop of less than 1 volt. A DC power switch was installed at each end of the cable to facilitate testing and pump priming. The cables were buried out of sight for the duration of the field trial.

The monitoring instruments and data acquisition system were installed at the same time. The photos in Figure 13 show the pressure transducer and flowmeter on the vertical pipe from the pump, and the two data loggers in their rain-tight enclosure mounted on the PV array trailer frame. The signal conditioning circuitry was behind the loggers in the same box. The battery powering the loggers is at the bottom of the box in the photo. After installation, the voltage, current, irradiance and temperature signals were all recalibrated. The pressure, speed and flow signals could not be easily checked.

After checking the plumbing, wiring and data acquisition, the pump system was started up on May 5. With the sun shining, but the power shut off, the pump was primed by pouring water down the discharge pipe until the pressure transducer showed a reading. The priming tap (visible at the top of the pump in Figures 12 and 13) was opened to release trapped air. The pump was started and stopped several times to clear out air from the impeller and suction pipe. When there was no more sound of trapped air, the pump was turned on and allowed to operate normally.

The data loggers were usually played back in the evening after the motor had stopped. Rather than return the loggers to TPK, the computer was taken to the site to play back and store the data. This minimized the down time for the loggers as well as travel to the site. Sometimes, all eight channels were logged for a period of one to four days. Mostly, however, only the solar irradiance, array voltage and flow were recorded, over four to ten day periods. After storing the data, it was reviewed to check for anomalies. Some of the data were analysed to ensure that the signals behaved as expected and to check that the insolation and pumped volume were reasonable.

After installation, and some initial "teething" problems, the pump and data acquisition systems both worked well, and collection of useful information began.

## 8.0 FIELD RESULTS

The complete system was in the field for a period of four months. Except for periodic adjustments to the discharge to maintain a constant static head, the system was left alone and allowed to operate automatically. At the end of June, the river level had dropped so far that the system had to be stopped to extend the suction pipe a further 13.7 ft (4.2 m). Unfortunately, the new joint leaked and the pump lost its prime, so that no pumping occurred for several days before the problem was rectified. After repriming the pump, the system worked normally again.

The data loggers recorded the system performance every day. Typical results for the eight channels were included in Figure 7. Most days were marred by scattered clouds. The loggers had difficulty recording the many resulting startups and shutdowns accurately. As a result, much of the data were compacted as depicted in Figure 8. The results for the clearest day (June 17) are plotted in the eight graphs in Figure 14. Each graph indicates the signal calibration and other pertinent data. This day represents the best possible in terms of both insolation and water pumping.

Referring to Figure 14, the solar irradiance plot is very close to ideal. The sun shines onto the array for almost 12 hours, peaking around noon at more than 1000 $W/m^2$, giving an insolation of 29.3 $MJ/m^2$. The array current plot has a similar shape. The array voltage plot has the expected shape as shown in Figure 10. The motor speed curve is almost identical, having the same characteristic "shoulder" which defines the start of flow. On the flow graph, there is no flowmeter signal between 0 and 5 Hz. Thus, the flow actually starts earlier and stops later than indicated. However, the amount of volume missed because of this is quite small, about $0.5\ m^3$. This is insignificant in the total volume of $90.76\ m^3$, but would be more important on dull days. The last two plots in the figure are the ambient and module temperatures. The perturbations in these curves are presumably caused by changes in wind velocity.

The pressure plot requires some explanation. The transducer was positioned above the pump, 3.15 m above the river level on that day. Thus, it only responded to water pressure above its level, giving no indication of total static pressure or dynamic head. Its results are, therefore, not very useful. A differential transducer between the pump inlet and outlet would have been better as it would have shown the total dynamic head. Nonetheless, the plot does reveal some interesting features. First, the pipe at the discharge end was leaky as

indicated by the pressure decay of about 60 cm in the hours following the shutdown of the system. The fact that this decay stops indicates where the leak was and that there were no other significant leaks in the rest of the plumbing. The discharge pipe filled up when pumping resumed in the morning, and the pressure at low flow represents the static head above the transducer. According to the signal, this pressure is 4.4 m of water, giving a total static head of 7.5 m, considerably more than the 7.0 m expected. It is unlikely that the height measurements made during system setup were so inaccurate. Rather, there was probably some offset drift in the transducer itself or in the signal conditioning circuitry.

More serious is the difference between the static head and the peak of the pressure signal. This represents the dynamic head loss in the top part of the discharge plumbing. According to the calculations [12], it should be only 14 cm, whereas the plot indicates 43 cm. This discrepancy cannot be due to the transducer. Rather, the theoretical calculations must somehow be in error. Perhaps some sources of friction were ignored or the pipes were partially blocked. The effect of this extra head on the results is discussed below.

Daily data from the field trial were analysed in several ways. The following set of figures are parametric plots of actual system operation compared with expected performance. Only unambiguous data for steady state operation on clear days were used to minimize scatter. The graph in Figure 15 is the array current vs. solar irradiance. The curve is non linear at the top end because of the shape of the array I-V curves around the maximum power point (see Figure 6). Up to 700 $W/m^2$, the current is as expected. Above this level, the reduced current may be due to module heating or the unexpectedly high dynamic head. There is also some slight hysteresis in the plotted data, between morning and afternoon. Ambient temperature differences, a slight angular mismatch between the array and the reference cell, temperature drift in the current shunt or other sensors, and the data storage format in the loggers could all contribute to this effect.

The expected and actual motor speed vs. array voltage are compared in Figure 16. The two agree very well except for some hysteresis. Note that the startup and shutdown thresholds differ by about 2.6% in speed. This is also apparent in Figure 14 and may be due to hourly variations in river level, water temperature and motor temperature changes, or to temperature drift in the voltage signal circuit. The electrical load line or current vs. voltage curve for the system is plotted in Figure 17. Again, except for the same hysteresis effects, the actual data is in good agreement with the expected performance.

In Figure 18, the instantaneous pump flow is plotted against irradiance for several days of data. Clearly the pump system did not perform as expected. Two effects are apparent. First, even in the June 17 data, there is less flow than expected at high sunlight levels. This is partly because of the lower current (Figure 15), but the high friction losses at high flow rates discovered above would also limit the maximum flow possible. Why this would not affect the previous parametric plots (Figures 15, 16 and 17) is not clear. Secondly, between July 21 and August, there was an apparent increase in startup irradiance which shifts the entire curve to the right, further reducing the flow at peak irradiance. The graph of net wire-to-water efficiency in Figure 19 reflects the same disappointing performance at high flow rates. These effects are discussed below.

In the last parametric plot (Figure 20), module temperature rise above ambient is plotted against irradiance. Wind variations and thermal lag in module heating cause the scatter seen in the actual data. Module heating is less than expected from Figure 11, possibly because the Almonte site was windier than the position behind TPK's Nepean plant. The data appear to reveal a linear relationship between module heating and irradiance, with a 24$^{o}$C temperature rise at full sun.

The logged results for each day were analysed to determine the total insolation, hours of operation and pumped volume for the day. The results are summarized in Tables VII through X, which represent a log of the entire field trial - one table for each month of operation. The tables also list the recording period and channels for each day and any events which occurred. In several rows, some of the records are in brackets, indicating that the value is incorrect or otherwise unusable as explained by the notes. In some cases, the record for the day was incomplete, in others, the data were compacted in the logger to the point where the integral became inaccurate.

On several days (note 4), the flow started later than it should have, as revealed by the voltage and irradiance plots for those days. These plots showed that the pump was turning at a higher than normal speed, without producing any flow. This would occur if the pump had lost its prime or if the suction or discharge pipes were blocked. Neither of these seems likely as, in all cases, normal operation resumed automatically within an hour or so. Thus, the true cause of these anomalies remains a mystery. The suction pipe extension and subsequent loss of prime are shown at the end of June in Table VIII.

Several times, after logging the data, the calibration of the irradiance signal was accidentally changed while

reprogramming the loggers (note 5 in the Tables). This change was subsequently discovered during the next logging period. Fortunately, it was possible to determine the new calibration form the data and correct for the error. Other days late in the summer had unexplained dips in the irradiance without affecting the voltage or flow (note 6). Notwithstanding these problems, most of the data were well behaved and could be readily analysed. The total and average results for each month are included in the Tables.

The performance of the pump system over the four month period is summarized in Figure 21 where daily pumped volume is plotted against insolation. The bracketed data points in the above Tables are excluded from this plot. The remaining data show a fairly close distribution around the central trend. Negligible water is pumped on dull days with less that 5 $MJ/m^2$ of insolation, and above 10 $MJ/m^2$, the trend is quite linear, with some scatter. The data points are identified by month. While a slight decrease from May to August is apparent, it is less that the scatter within any one month. This indicates that the data selected for Figure 18 were perhaps not representative and that there was not a marked degradation in system output during the four months.

The specified design target of 60 $m^3$/day is shown in Figure 21. The 18 $MJ/m^2$ on a horizontal surface has been adjusted for the array angle. Based on the results shown, the system appears to be short of the design goal. This is a reflection of the lower-than-expected efficiency seen in Figure 19. It may be partially due to the high dynamic pressure losses discussed above. A higher head would result in a lower flow. Two other reasons for the reduced performance were discovered after the field trial (see Section 9).

The last recorded day was September 1, 1987. Prior to this, several of the sensor calibrations were checked and the entire system was inspected for leaks and damage. The next day, the system was disassembled and returned to TPK for testing and evaluation.

## 9.0 EVALUATION AND DISCUSSION

After a cursory inspection of the plumbing and major components, the pump/motor subsystem was installed at TPK for retesting. The pump and motor were neither cleaned nor disassembled. Testing was performed with the pump set up as before (refer to Figure 4). At first, the motor current, shaft speed and discharge pressure were measured over a wide range of voltages, with the pump in cutoff (zero flow). This test is a good indicator of mechanical losses in the subsystem. The motor speed and pump pressure were very close to the original (pre-trial) results. As shown in Figure 22, however, the current was quite different. Over the entire voltage range, the current increased by an almost constant amount (about one ampere). Such a shift is caused by an increased motor torque required to overcome an additional friction on the shaft.

Such an increased parasitic load on the shaft is one reason for the performance of the system in the field being lower than predicted. It accounts for the shift in startup threshold seen in Figure 18, and some of the efficiency reduction. To determine if the friction was in the motor or the pump, the motor was checked with the pump seal and impeller removed, after testing the pump. The no-load motor current over a wide range of speeds was much the same as found during the original motor tests. Thus, the motor efficiency was judged to be unchanged and the friction had to be in the pump.

The pump was also tested over a wide range of flows at a fixed shaft speed of 1800 RPM. The head and efficiency results as a function of flow are plotted in Figure 23. During these tests, the calibration of the flow meter was re-checked. Up to 2 L/s, it was about the same as before, but above 2.5 L/s, it was found to be reading about 6% lower (in flow) than prior to the field trial. This is the second reason why the field trial results were lower than expected. It is unclear why its calibration should change in this manner. Perhaps the thin film of silt that covered all internal wetted surfaces slowed down the rotation of the paddle wheel at high flow rates. An error of this size, in so fundamental a parameter as the flow, clearly has serious effects on the accuracy of testing and the field trial results!

To determine what was causing the increased friction in the pump, it was disassembled one piece at a time from the suction end and carefully inspected for signs of rubbing or wear. There was, of course, some rust on the internal iron surfaces, but nothing abnormal. The epoxy on the inside of the casing was in good condition. The impeller had a thin coating of silt but was otherwise unaffected, with no obvious signs of

wear. When the seal was removed, however, it was found to have grease on both its carbon and ceramic faces. Light grease had been put on the shaft (as recommended by the manufacturer) to help the tight fitting rubber seal cup slip on. During the summer, it must have found its way to the seal faces where it prevented the normal water lubrication and thus increased the seal friction.

After cleaning the grease off, the pump was reassembled without cleaning or adjusting any other part of it. It was then retested as above and the results are plotted in Figures 22 and 23. For the most part, they are the same as or slightly better than the original results. Thus, it appears that the entire efficiency reduction can be attributed to the greasy seal.

The motor was also inspected. No corrosion or obvious wear was discovered. The insides were coated with graphite powder from the brushes. These had worn down about 3.0 mm since March and had about 17.5 mm of useful length remaining. The pump system had run 117 days, or about 750 hours, during the field trial. Thus, the expected total brush life would be 5,000 hours or 26 months of field use.

Taken together, the grease on the seal and the inaccurate flowmeter account for the lower-than-expected results for the field trial. The increased friction led to a high startup current threshold and thus reduced the pumping period during a typical day. The friction also reduced the pump efficiency at all flow levels. The erroneous flowmeter readings at high flow levels further degraded the apparent efficiency. It is difficult to accurately calculate the result of these two effects on the total pumped volume for a typical day because the system is non-linear. However, by way of an example, an estimate can be made as follows.

From Figure 15, at the 800 $W/m^2$ design point, the actual array current was 5.85 A. From Figure 22, 16% of this current was needed to overcome the excess seal friction. At this same irradiance, the apparent flow was more than 2 L/s so that the flowmeter must have been reading about 6% low. If neither of these effects had occurred, therefore, the flow would have been about 26% higher than that shown in Figure 18 at this irradiance - very close to the expected value. If the same factor is applied to the apparent pumped volume at the specified insolation from the curve in Figure 21, a volume of 64 $m^3$ is found - again, close to the 60 $m^3$/day design goal. Thus, it appears that the system would have met the specifications if the manufacturer's recommendation of using grease to aid in installing the seal had not been followed.

## 10.0 CONCLUSIONS AND RECOMMENDATIONS

A shallow-well photovoltaic powered water pumping system was designed, constructed and tested in the laboratory and outdoors. It was then subjected to a four month field trial. While the system initially performed as expected, in long term field use, the daily volume design goal was not met. This was partly because the plumbing friction losses were higher than anticipated, but mostly due to the presence of grease on the pump seal. This increased the seal friction and reduced the pump efficiency.

Each of the system components was characterized in the lab. The testing was straightforward, but accurate calibration of the monitoring instruments was troublesome. Also, reducing the data to a useful format was quite tedious. The paddlewheel type flow meter was especially disappointing, being non-linear and subject to long term drift. As expected, the single-stage, centrifugal pump efficiency was lower than reported by the manufacturer, but still quite good, with a maximum of 65%. The permanent magnet DC motor performed as specified, with an operating efficiency around 85%. In laboratory testing, the overall system operated as expected from the design calculations, validating the design procedures.

The outdoor winter testing was not worthwhile in terms of obtaining useful system data, because of the effects of the antifreeze on the system hydraulics and the effects of low temperatures on the motor and PV array. This testing did, however, serve to debug the monitoring circuitry and determine the characteristics and limits of the data loggers. Indeed, most of the technical problems encountered during the project involved the monitoring instrumentation. It was difficult to ensure that the sensors were functioning and generating accurate test data. On the other hand, the PV supply for the data acquisition system proved quite adequate and reliable.

Although field trials are the last step in development of a product, some additional work could be done to improve PV pumping systems. This includes study of the loss mechanisms to determine how the overall system performance can be improved, and additional field trials and demonstration projects with permanent installations in a variety of real applications, in order to gain further field experience and raise public awareness of the technology. More reliable instrumentation for measuring flow and pressure should be sought. Finally, the analysis techniques for laboratory and field data reduction, while good, could be improved further.

In conclusion, the results of the field trial in general were very satisfactory. They have demonstrated that a PV pump system of the type studied here will operate reliably for extended periods when properly installed in the field.

## REFERENCES


1. J.A. Roger, "Water and Photovoltaics in Developing Countries". Solar Cells, Vol.6, pg. 295, 1982.

2. Sir William Halcrow and Partners, "Small-Scale Solar-Powered Irrigation Pumping Systems: Technical and Economic Review", UNDP Project GLO/78/004, September 1981, London England. Chapter 2.

3. W. A. Brainard, "The Worldwide Market for Photovoltaics in the Rural Sector", 16th Photovoltaic Specialists Conference, San Diego, Sept. 1982, pp. 1308-13.

4. Photovoltaics - Technology, Industry and Market Development Opportunities", Ontario Ministry of Energy Report, Ref. No. 301-8133, March 1983.

5. R.E. Thomas, et al. "Development of a Photovoltaic Powered Pumping System", Final Report, NRC/DSS Contract No. 0SX80-00098, March 1982.

6. C.E. Norman, C. Robins and B.G. Keefer, "Development of a Photovoltaic Powered Shallow Well Pumping System", Final Report NRC/DSS Contract No. OSX83-00162, Nov. 1984.

7. C.E. Norman, D.G. MacKenzie and C.J. Robins, "Photovoltaic Water Pump Development", Report on Technology Development, Ontario Ministry of Energy, Contract No. 809-8205, August 1984.

8. J. Larocque, J. Savage, J.L. McClung and M. Westcott, "Development of a Facility for Evaluating Small Photovoltaic Powered Water Pumping Systems", Final Report ES/EDP-85-13, NRC/DSS Contract No. 01SX.31926-3-3027, 1985.

9. J.F. Schaefer, "Results of a Survey of 110 Photovoltaic Water Pumpers in New Mexico", 18th Photovoltaic Specialists Conference, Las Vegas, pp. 858-865, October, 1985.

10. Sir William Halcrow and Partners and Intermediate Technology Power Ltd., "Small-Scale Solar-Powered Pumping Systems: the Technology, its Economics and Advancement", Main Report, UNDP project GLO/80/003, London, England, June 1983.

11. C.E. Norman, D.G. Harris, "Test and Evaluate High Efficiency Modular Power Conditioning Systems for Photovoltaics", Final Report NRC/DSS Contract No. 0SX82-00049, July 1984.

12. F.M. White, Fluid Mechanics, McGraw Hill, New York, 1979.

13. Hydraulic Institute Standards for Centrifugal, Rotary and Reciprocating Pumps, 14th Edition, Hydraulic Institute, 1983.

14. R.W. Matlin, "Design Optimization and Performance Characteristics of a Photovoltaic Microirrigation System for Use in Developing Countries", U.S. D.O.E. Contract No. EY-76-C-02-4094, 1979.

15. R.H. Perry, et al. editors, Chemical Engineer's Handbook, 5th Edition, McGraw-Hill, New York, 1973.

16. C.E. Norman, "Modelling Thermal Dissipation in Semiconductor Devices", B.A.Sc. Thesis, University of Toronto, 1974.

# APPENDIX A

## FIGURES AND TABLES

## FIGURES AND TABLES

### FIGURES


Figure 1. Block diagram of a direct-connected PV powered water pumping system showing important operation parameters.

Figure 2. Data acquisition system schematic diagram.

Figure 3. Steady state characteristics for Reliance 1/2 HP 90 V 2500 RPM permanent-magnet DC motor.

Figure 4. Laboratory testing of centrifugal pumps.

Figure 5. Measured head vs flow characteristics for the Leitch pump.

Figure 6. I-V curves for the photovoltaic array.

Figure 7. Sample data plots from pump system data logger for December 8, 1986.

Figure 8. Eight channels of data recorded over a period of six days showing effects of data compaction in three channels.

Figure 9. Calculated operating characteristics of type "B" pump system.

Figure 10. Simulated operation of pump system during a standard solar day.

Figure 11. Module heating as a function of sunlight intensity.

Figure 12. Installation of photovoltaic pumping system showing pump assembly and PV array.

Figure 13. Installation of PV powered pumping system showing pump plumbing with sensors and data loggers.

Figure 14. Sample data plots for the pump system in the field on June 17, 1987.

Figure 15. Parametric plot of array current vs irradiance for field data recorded on June 17, 1987.

Figure 16. Parametric plot of motor speed versus array voltage for June 17, 1987.

Figure 17. Pump system load line, or parametric plot of current versus voltage for June 17, 1987.

Figure 18. Pump system productivity: parametric plot of flow versus irradiance for three days in 1987.

Figure 19. Parametric plot of subsystem efficiency versus irradiance for field data recorded on June 17, 1987.

Figure 20. Parametric plot of module heating versus irradiance for clear days in 1987.

Figure 21. Summary of daily results for four months of PV pump system field trial.

Figure 22. I-V curves for pump/motor subsystem in cutoff (no flow).

Figure 23. Pump characteristics at 1800 RPM before and after field trial.

**TABLES**

Table I. Measured output for each of the available SW3804 modules at 1000 $W/m^2$ and 25°C.

Table II. Signal calibrations for data acquisition system.

Table III. Sample data readings for March 13, 1987 (simulated static head).

Table IV. Operating record for outdoor testing November-December, 1986.

Table V. Sample data listings at ten minute intervals for two channels from the data loggers, recorded on December 8, 1986.

Table VI. Calculated operating points for the pump system in steady-state operation at 7.0 m static head and 25°C ambient.

Table VII. Summary of field trial results for the month of May.

Table VIII. Summary of field trial results for the month of June.

Table IX. Summary of field trial results for the month of July.

Table X. Summary of field trial results for the month of August.

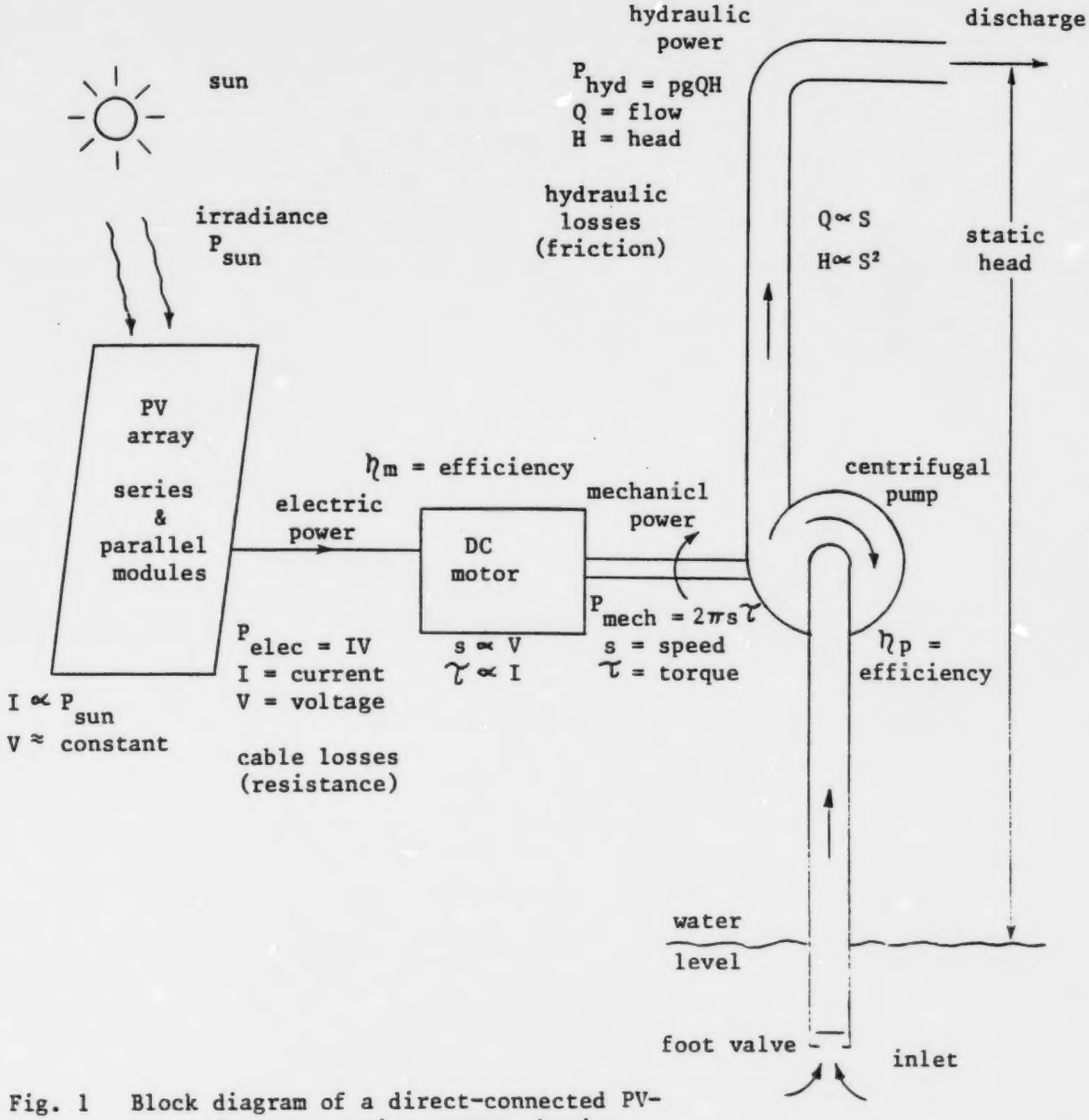


Fig. 1 Block diagram of a direct-connected PV-powered water pumping system showing important operation parameters.

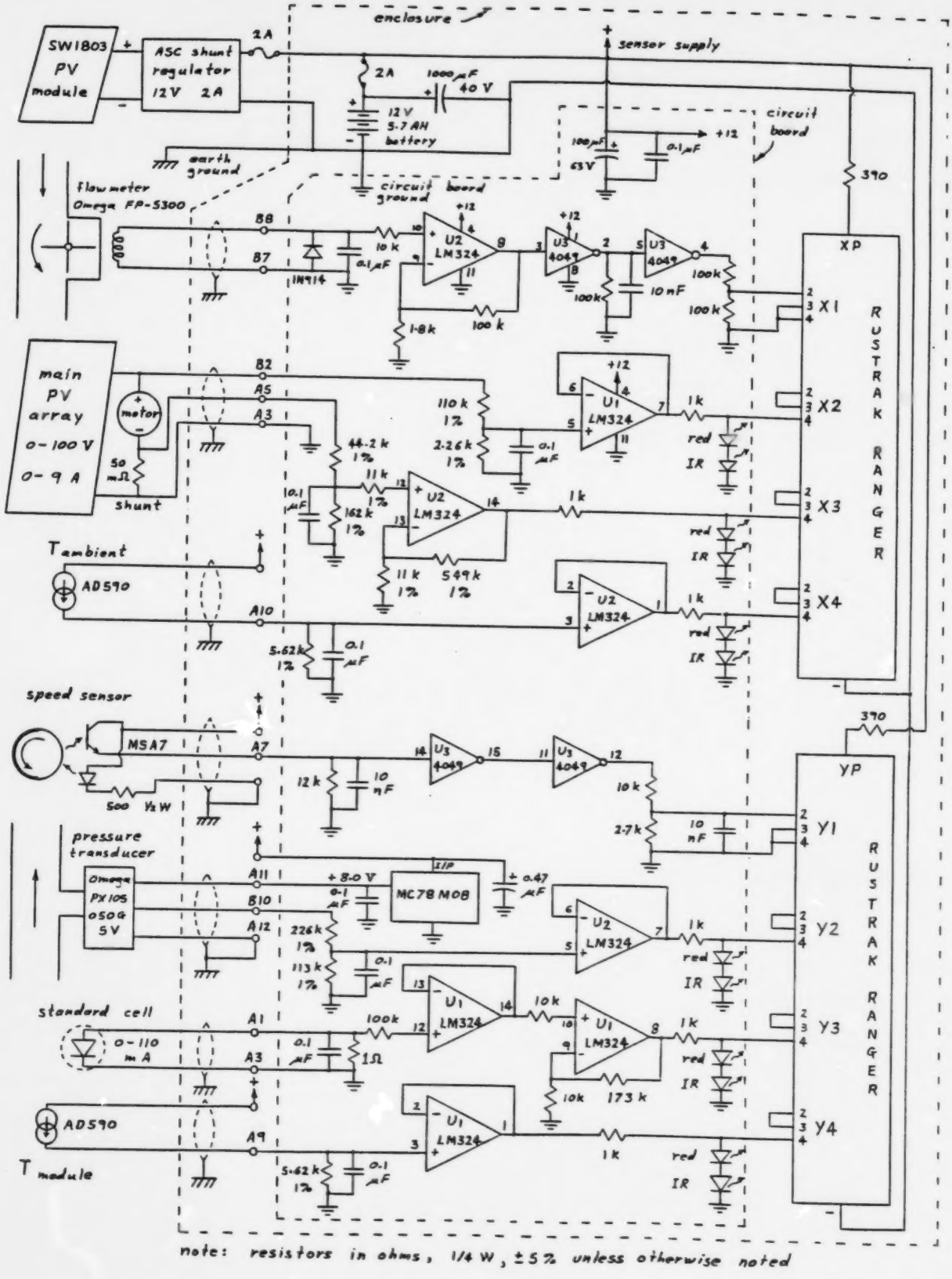


Fig. 2 Data acquisition system schematic diagram.

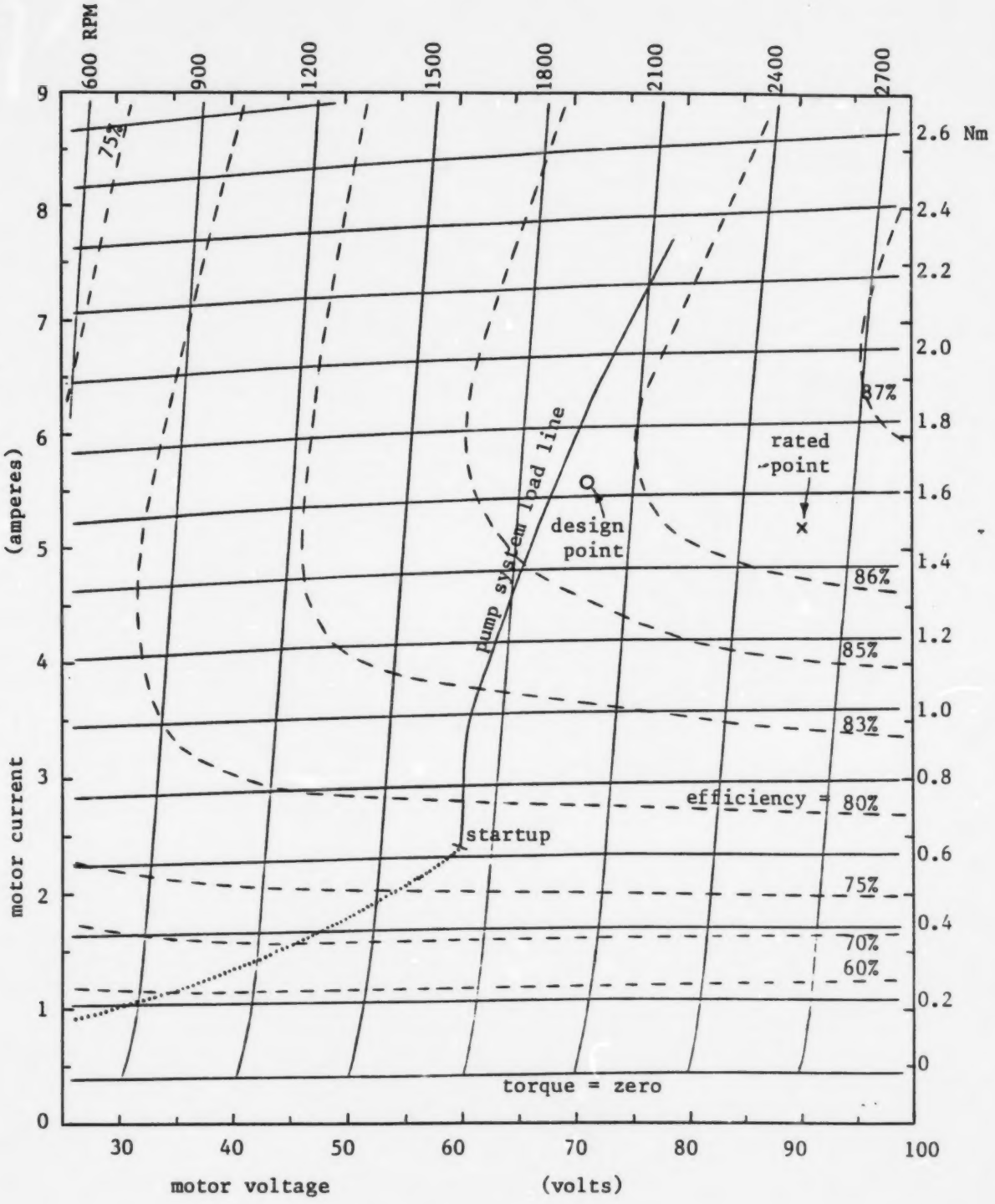


Fig. 3 Steady state characteristics for Reliance 1/2 HP 90V 2500 RPM permanent-magnet DC motor.

Fig. 4 Laboratory testing of centrifugal pumps.

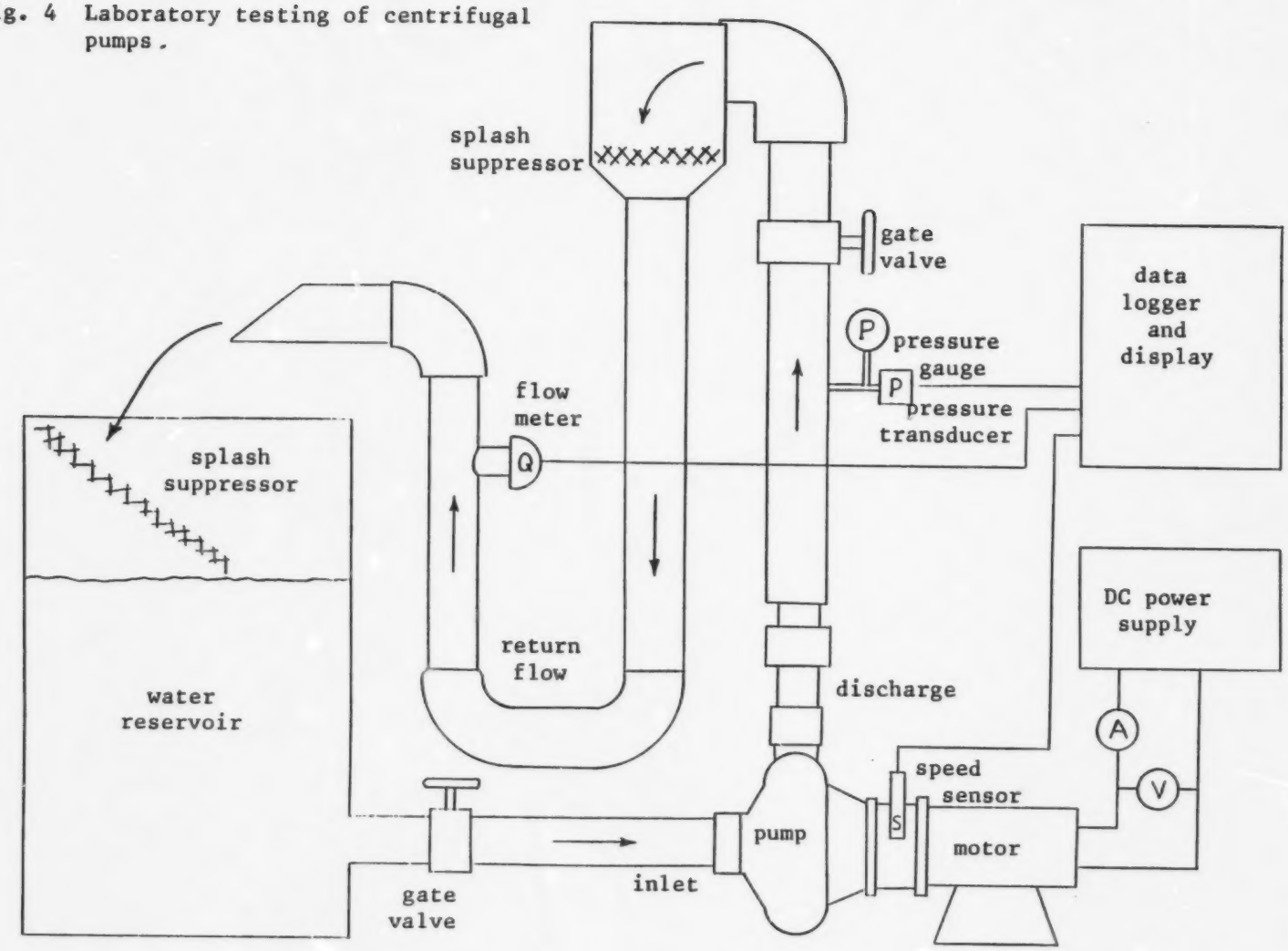

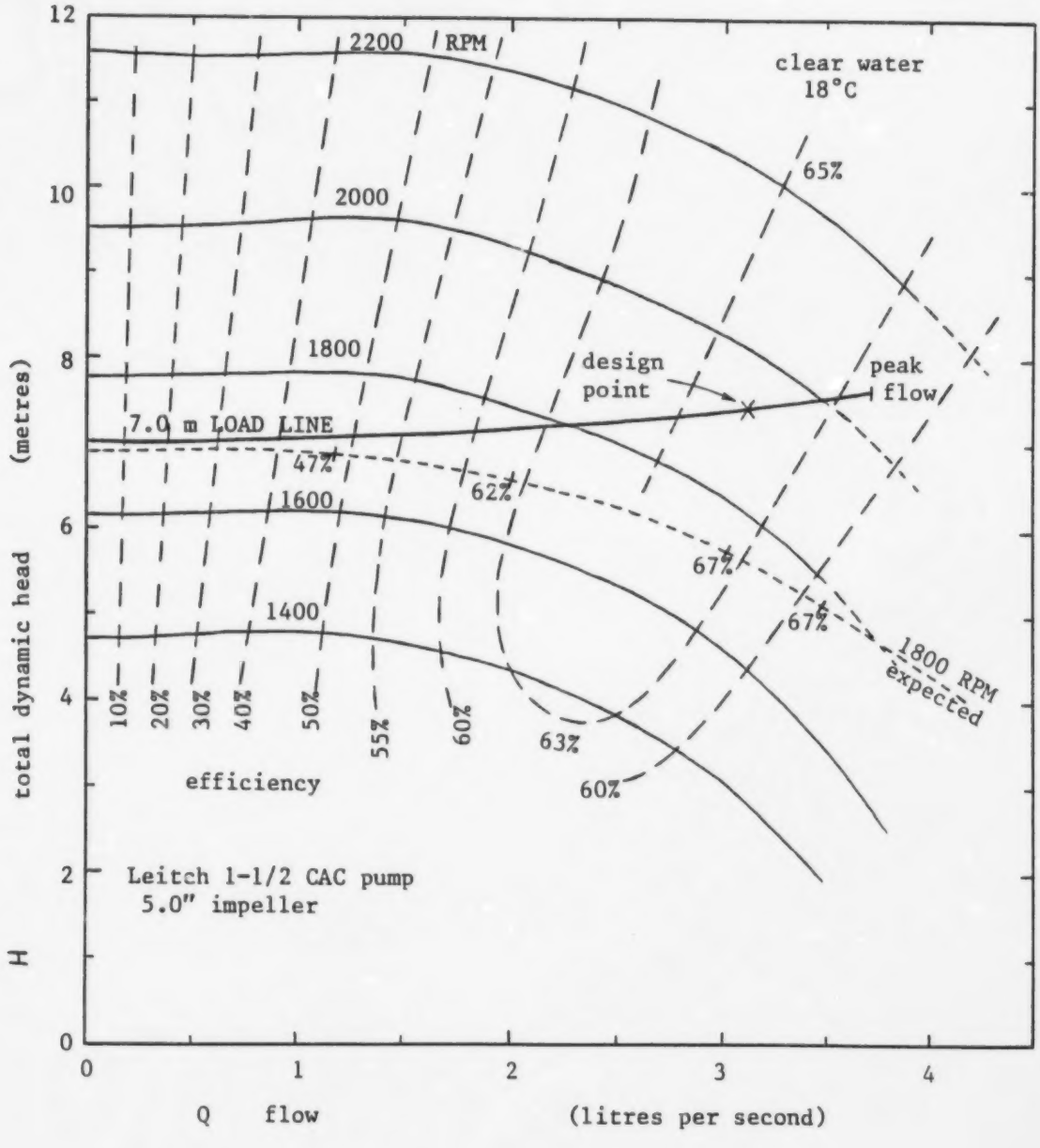


Fig. 5 Measured head vs flow characteristics for the Leitch pump.

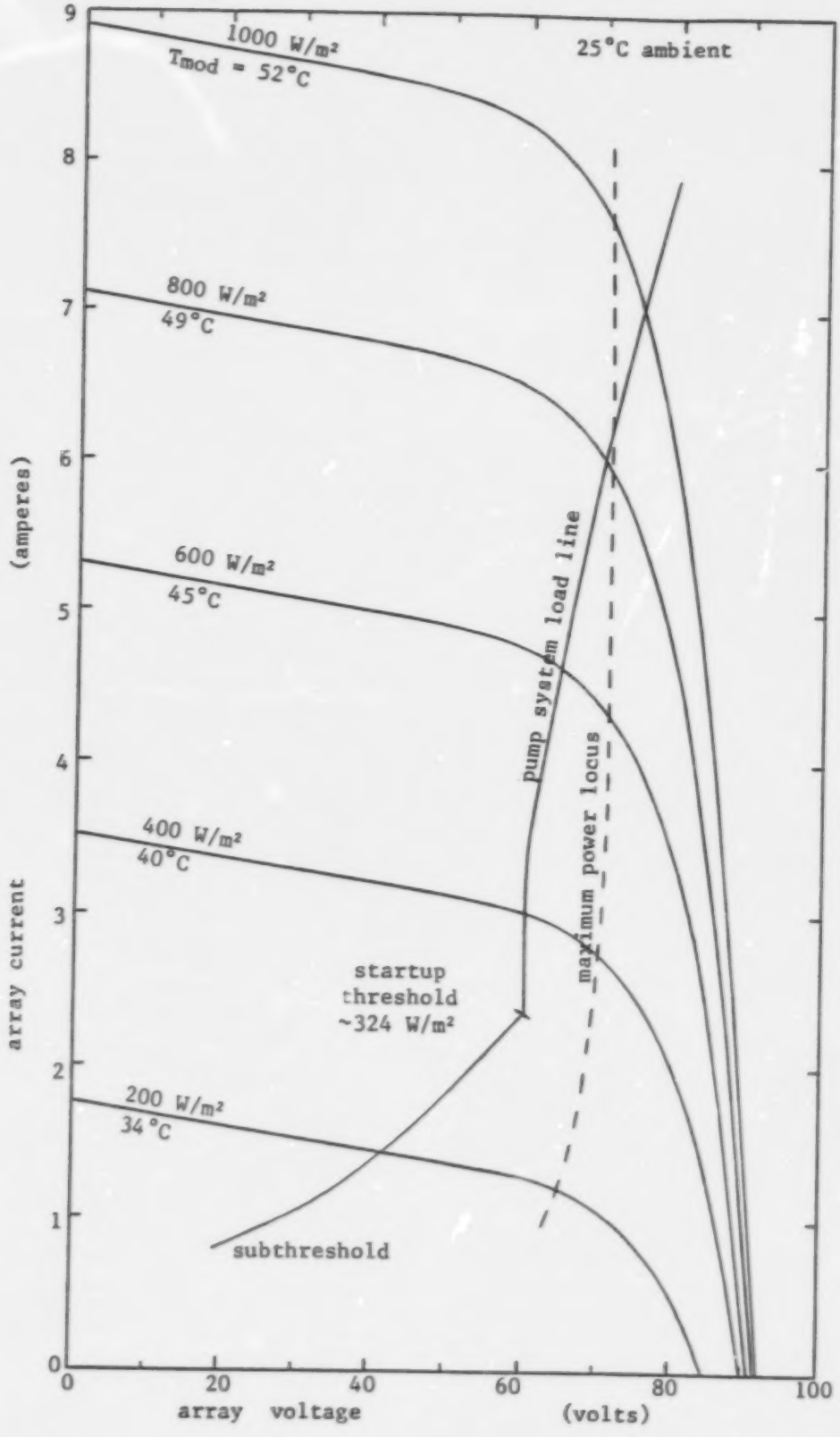


Fig. 6 I-V curves for the photovoltaic array.

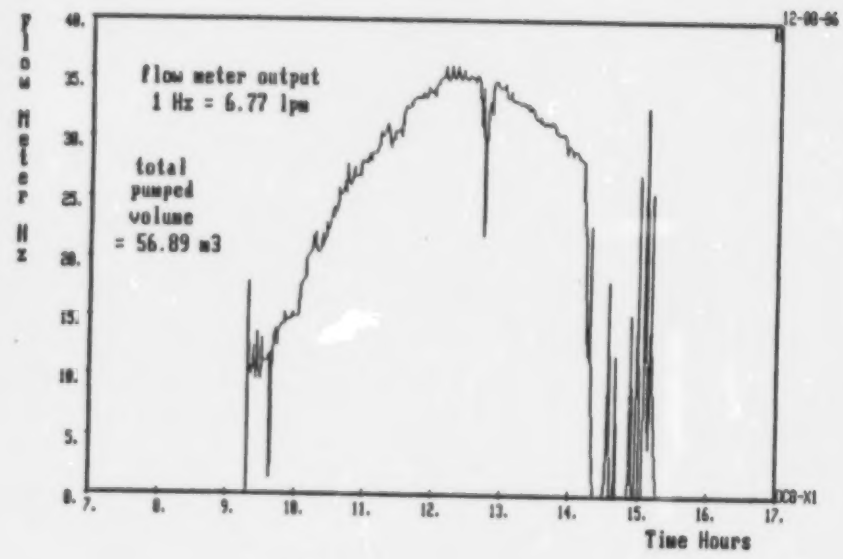


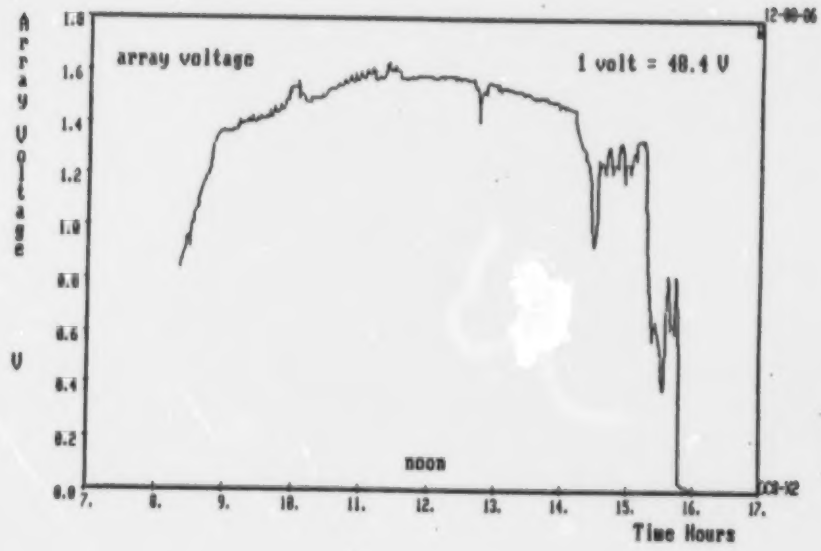


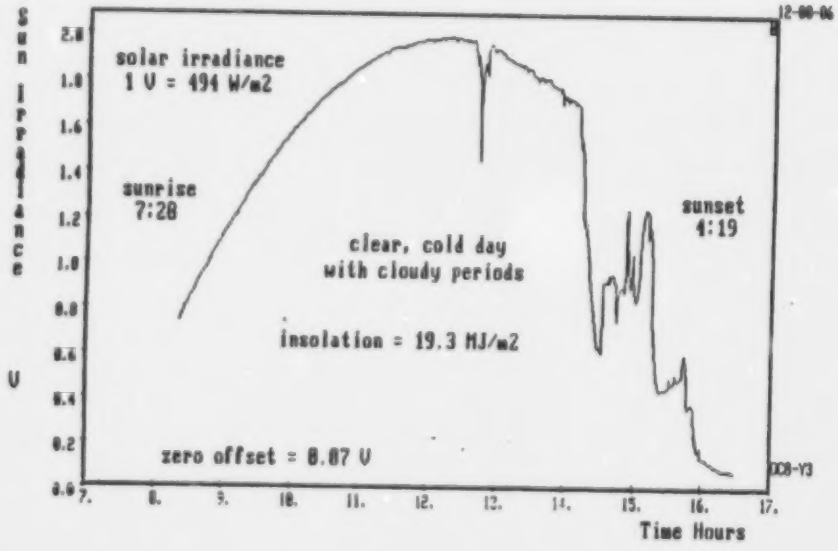


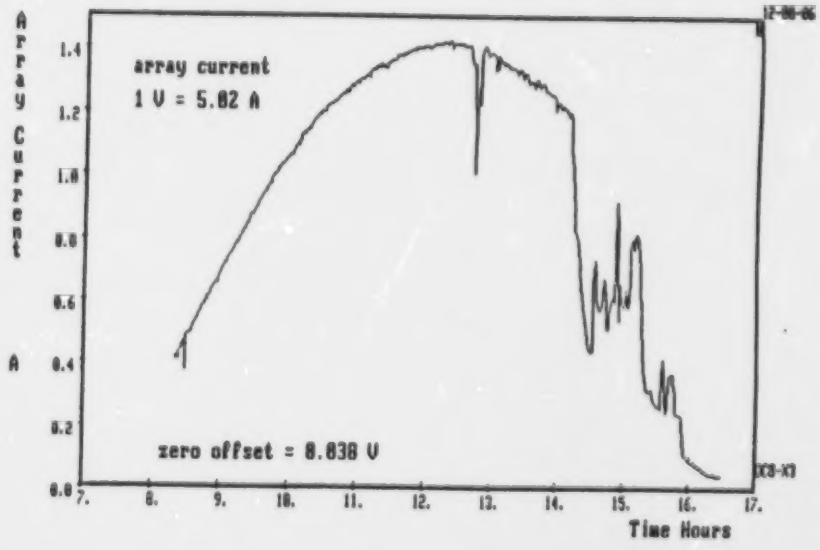


Figure 7: Sample data plots from pump system data logger for December 8, 1986.

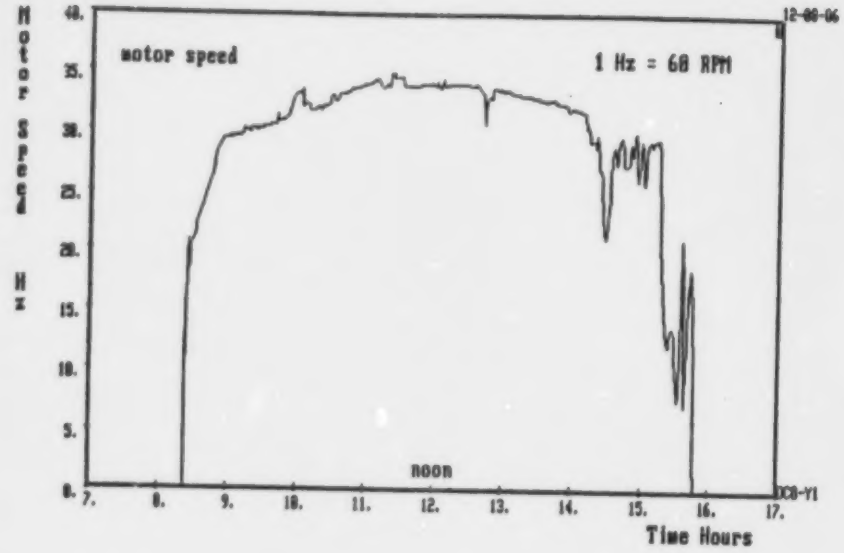


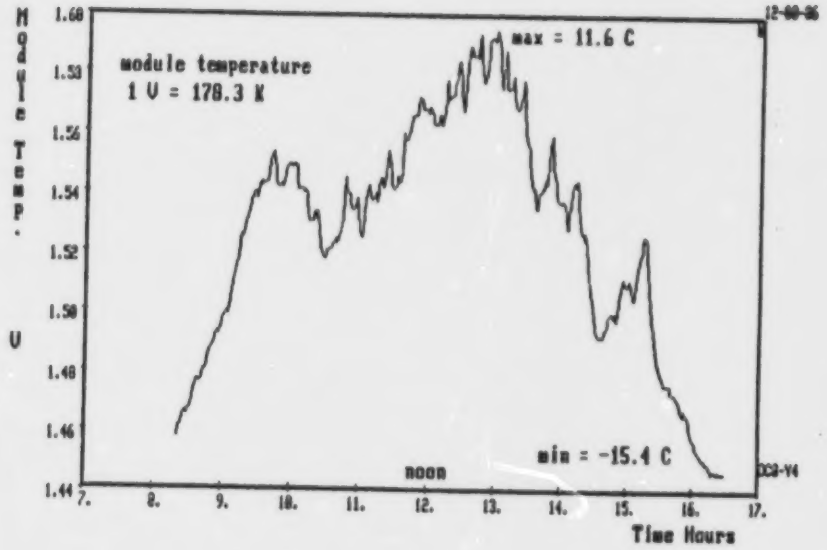


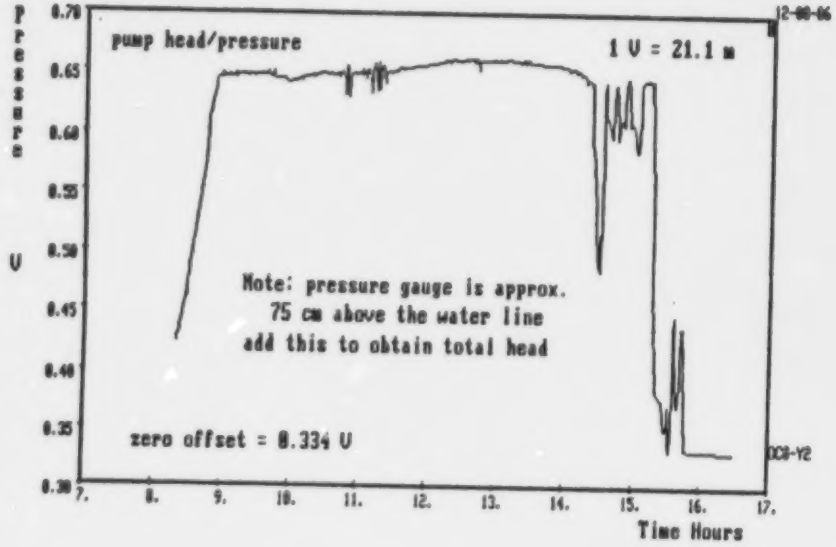
pump head/pressure
1 V = 21.1 m
Note: pressure gauge is approx.
75 cm above the water line
add this to obtain total head
zero offset = 0.334 V
Pressure V
Time Hours

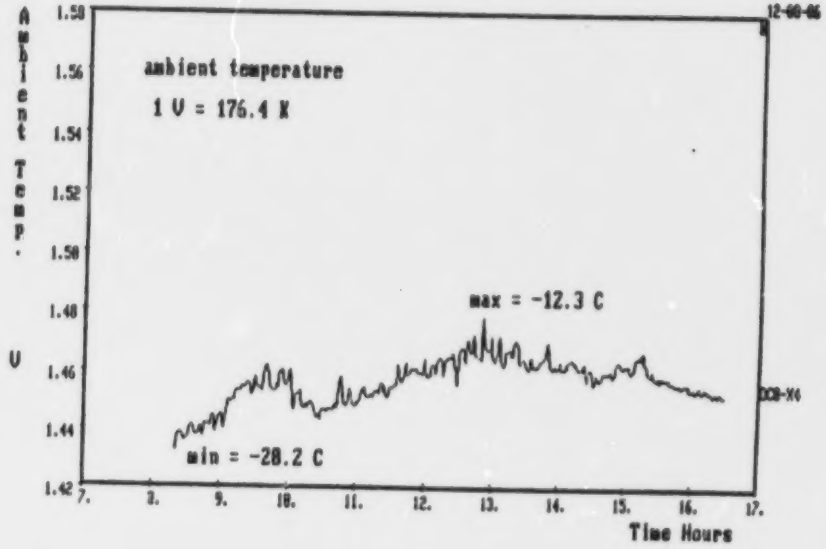


**Figure 7 continued:** Sample data plots from pump system data logger for December 8, 1986.

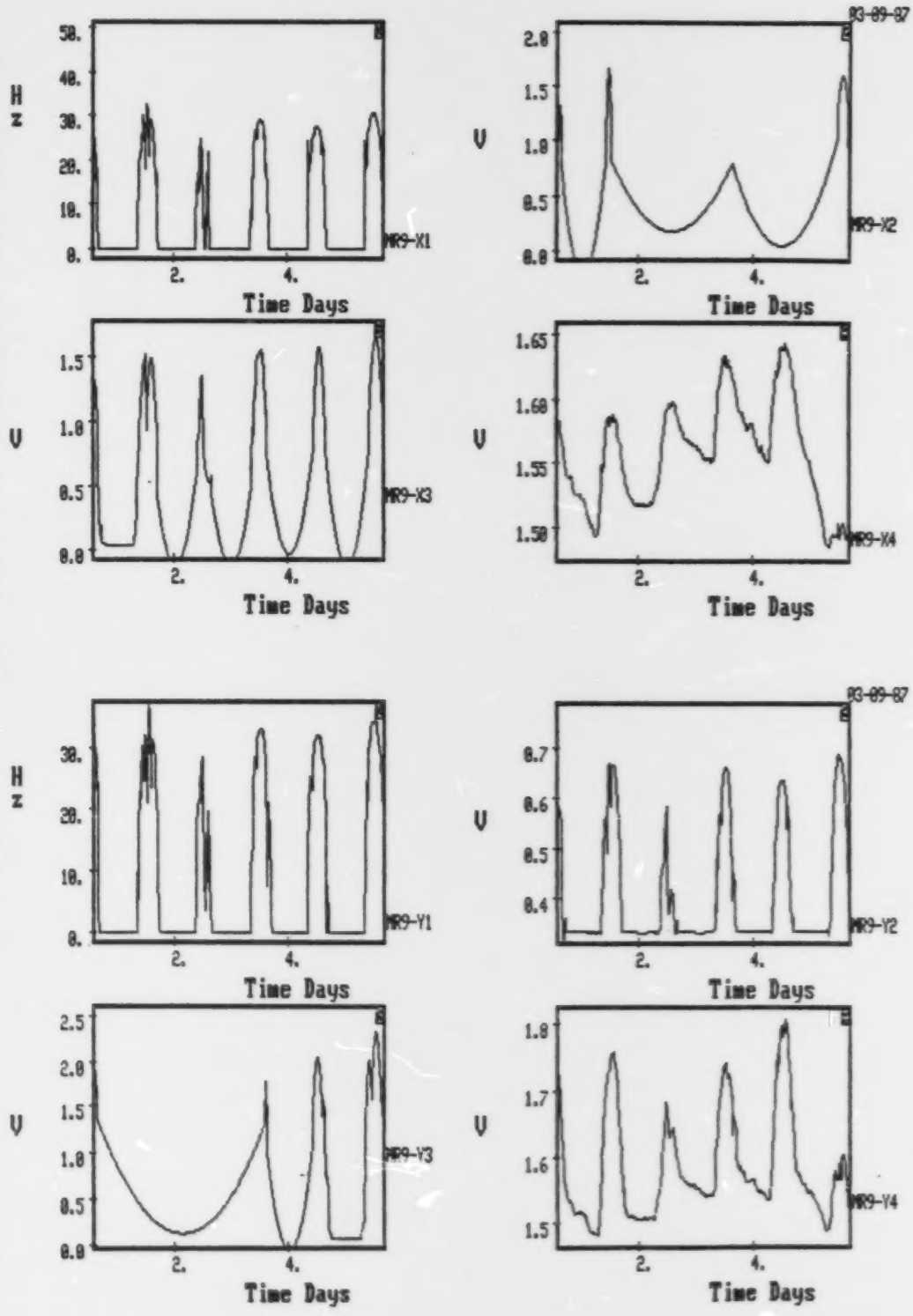


**Figure 8:** Eight channels of data recorded over a period of six days showing effects of data compaction in three channels.

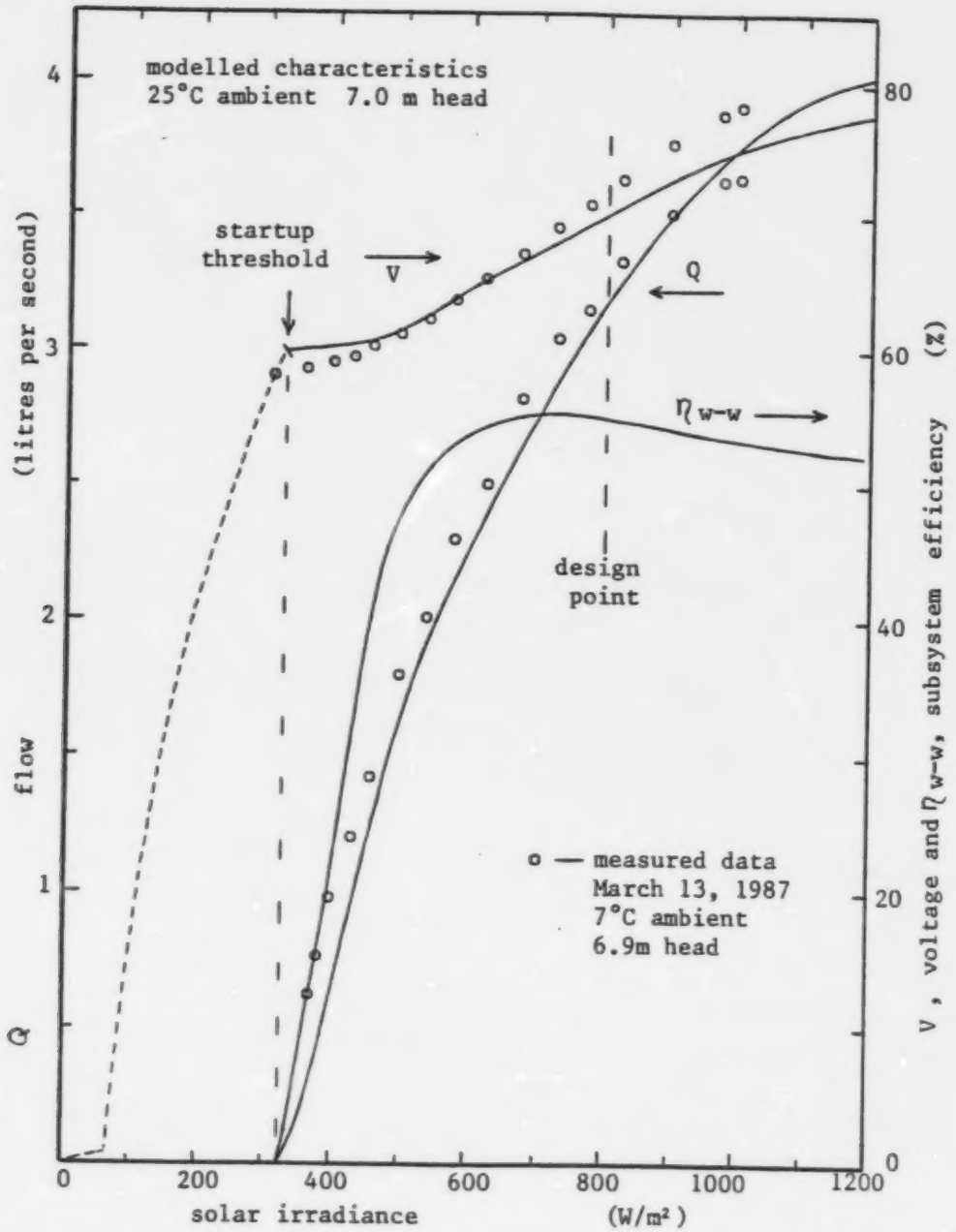


Fig. 9 Calculated operating characteristics of type "B" pump system.

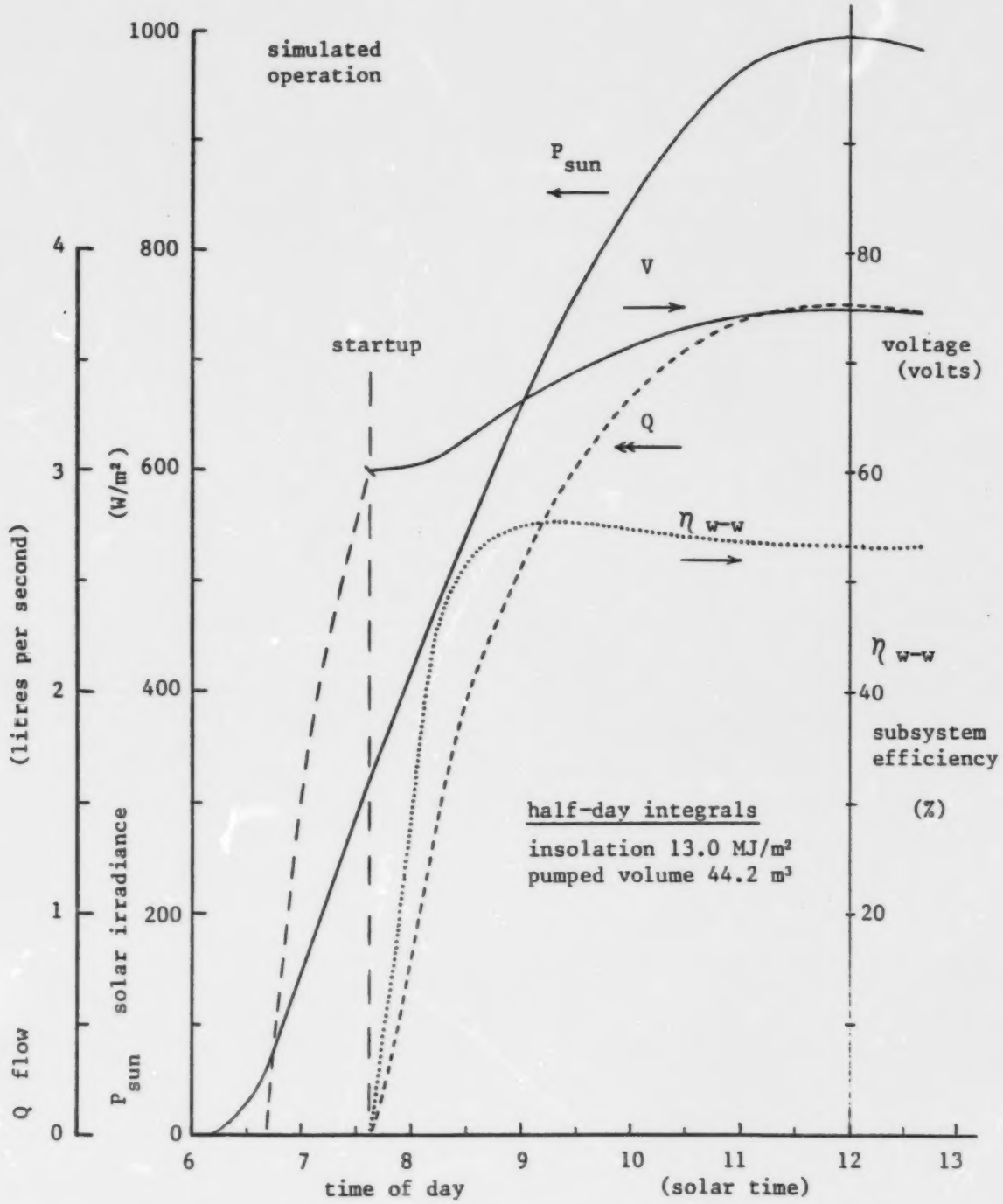


Fig. 10 Simulated operation of pump system during a standard solar day.

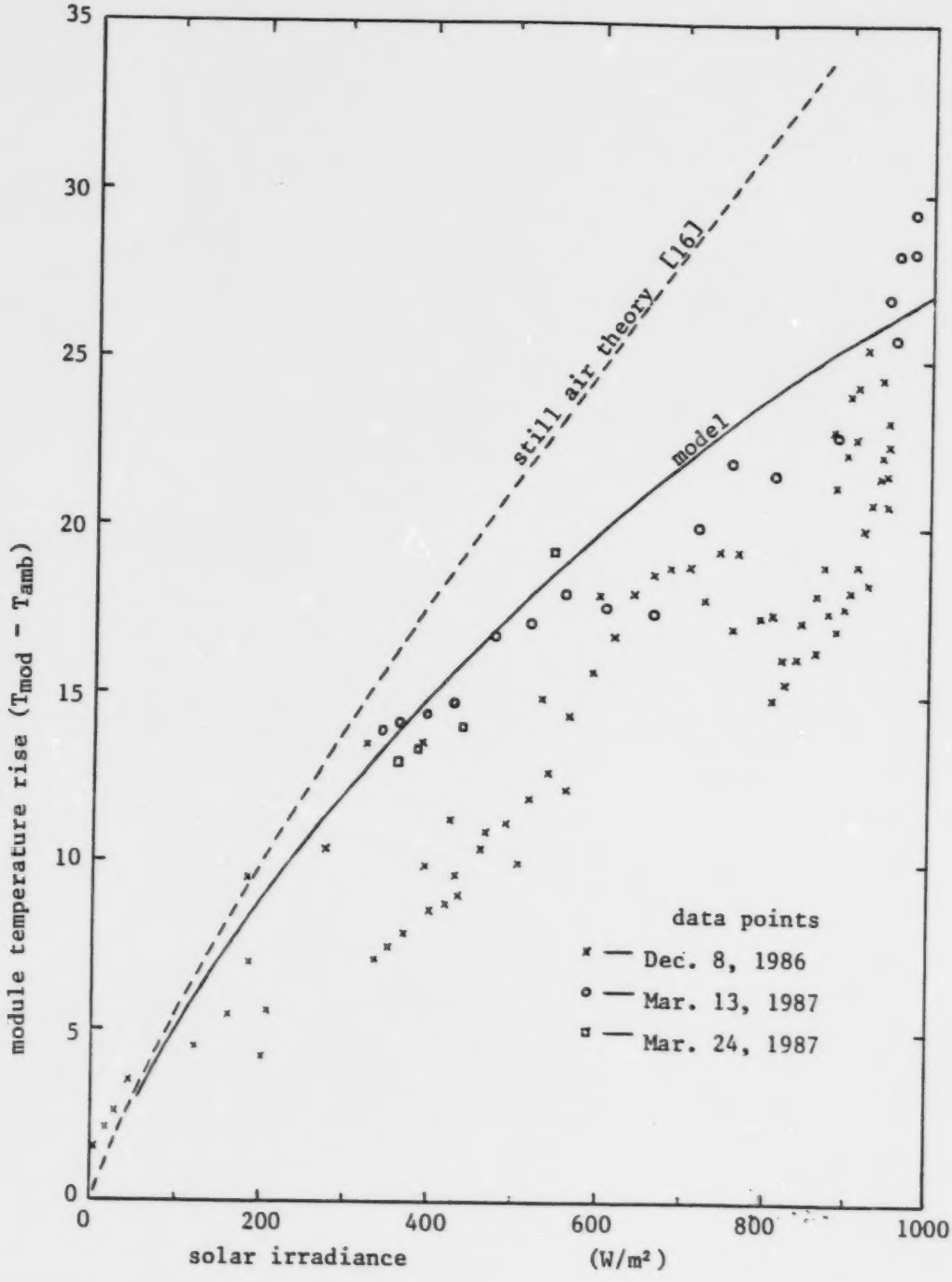


Fig. 11 Module heating as a function of sunlight intensity.

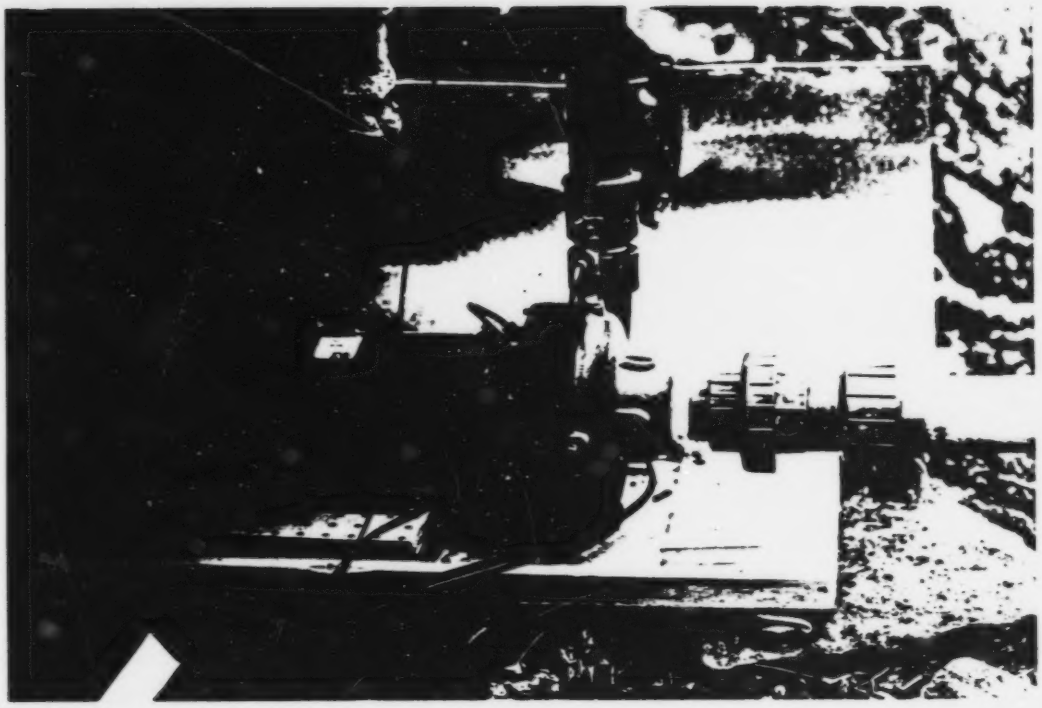

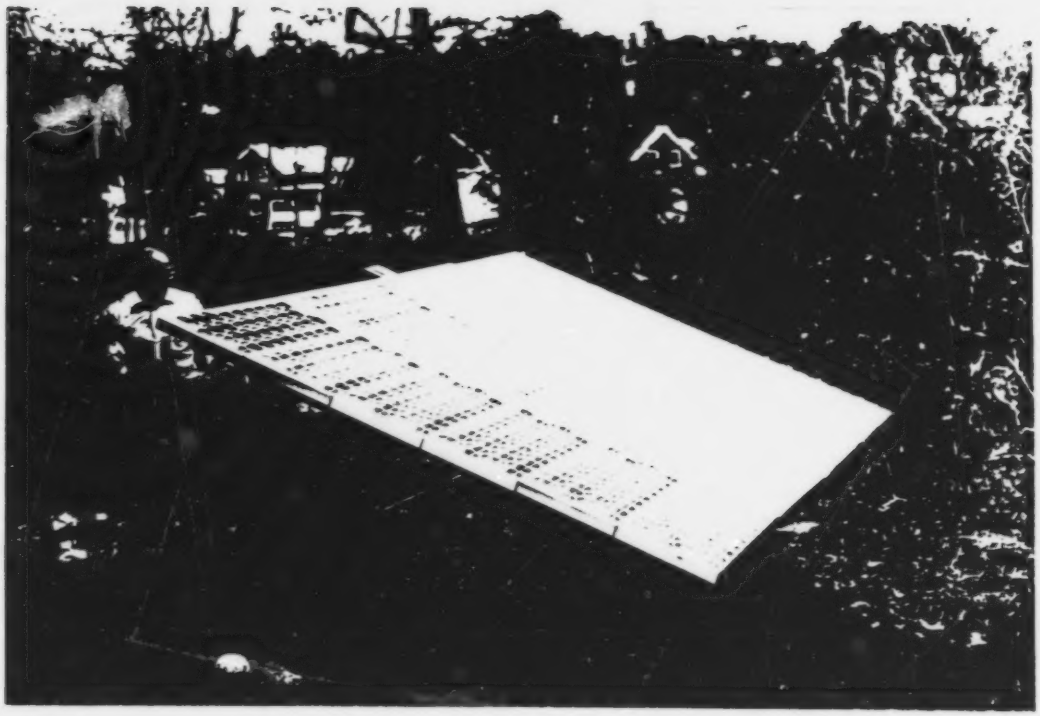

Figure 12. Installation of photovoltaic pumping system showing pump assembly (top) and PV array (bottom).

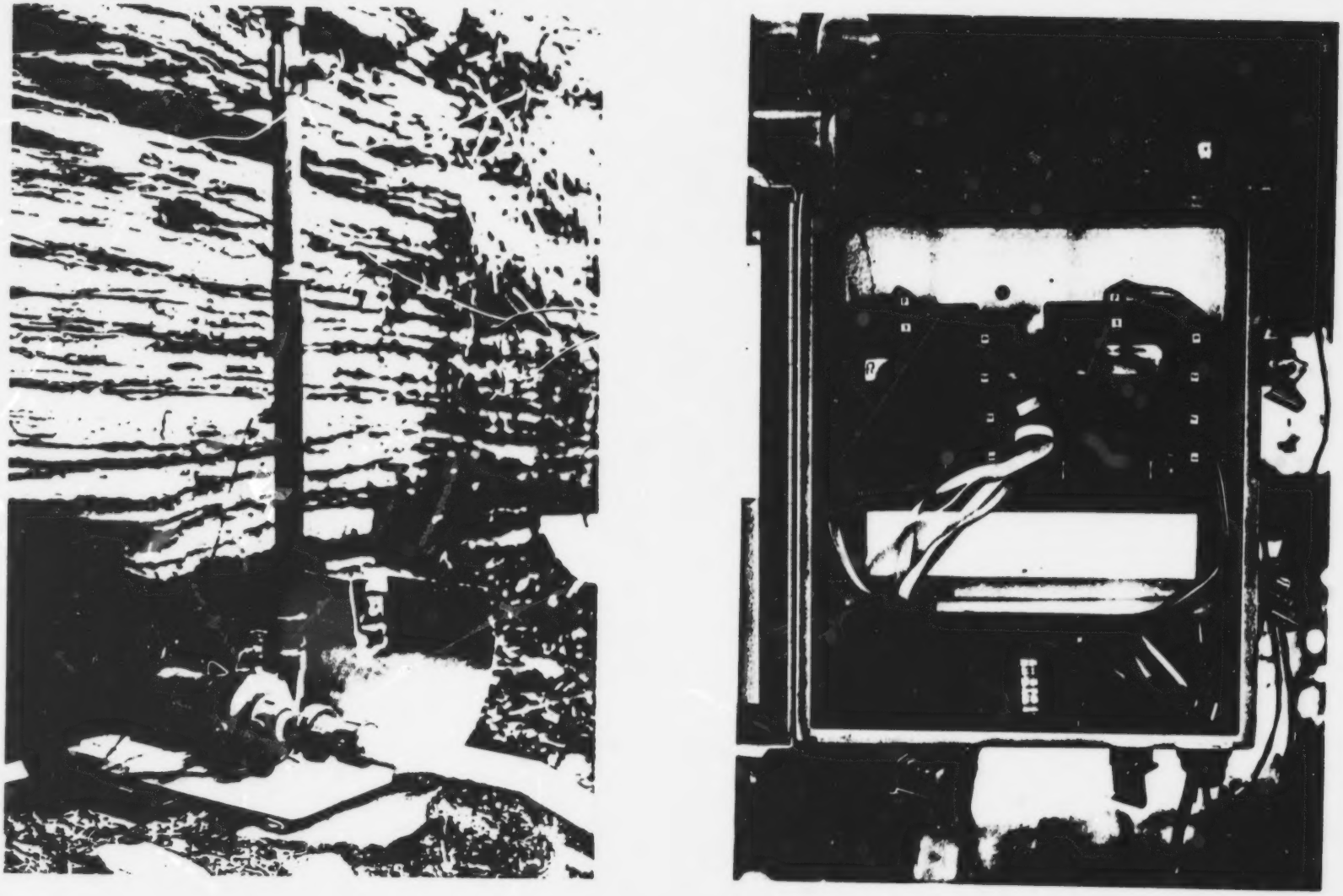

Figure 13. Installation of PV-powered pumping system showing pump plumbing with sensors (left) and data loggers (right).

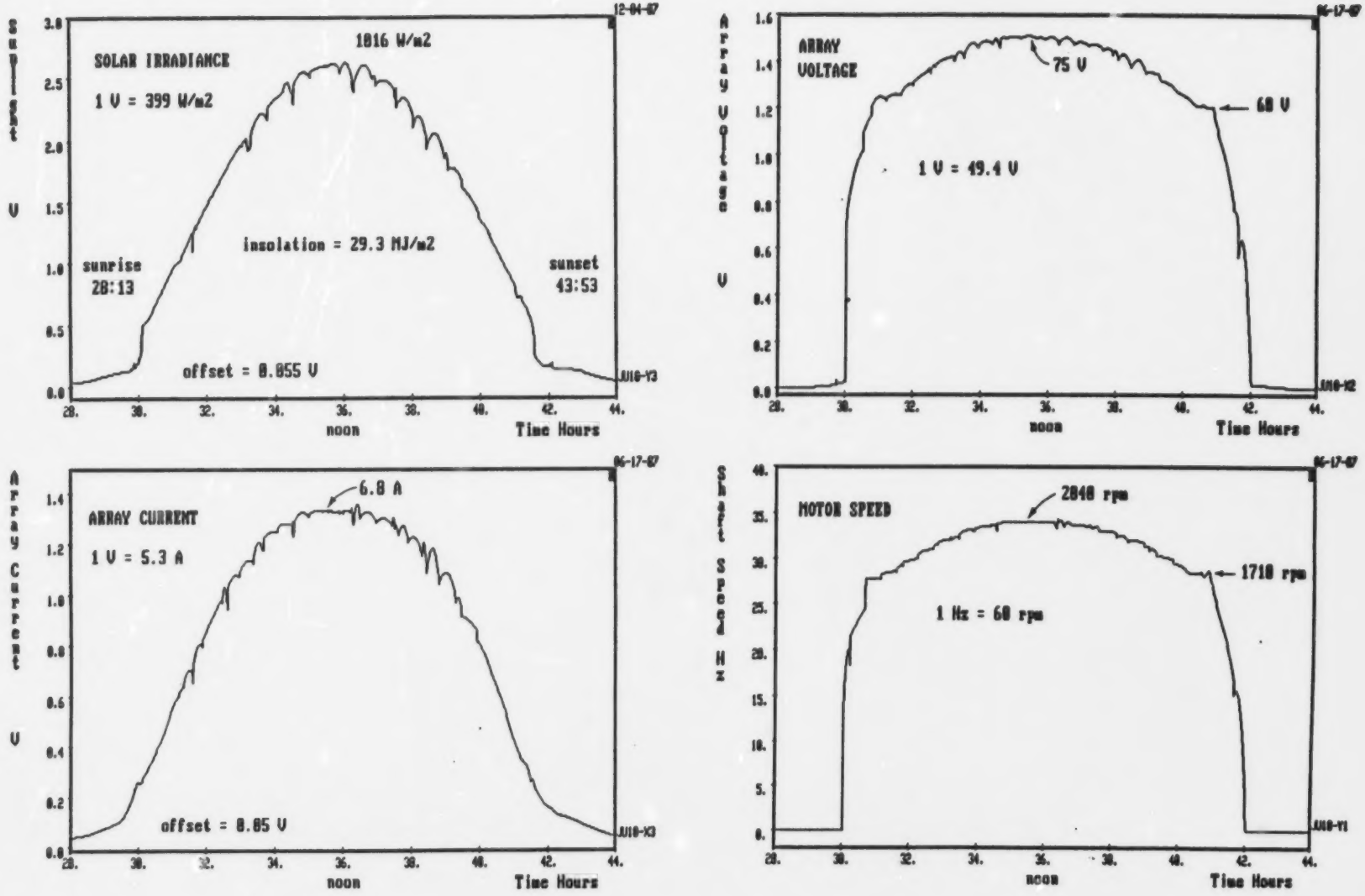


Figure 14. Sample data plots for the pump system in the field on June 17, 1987.

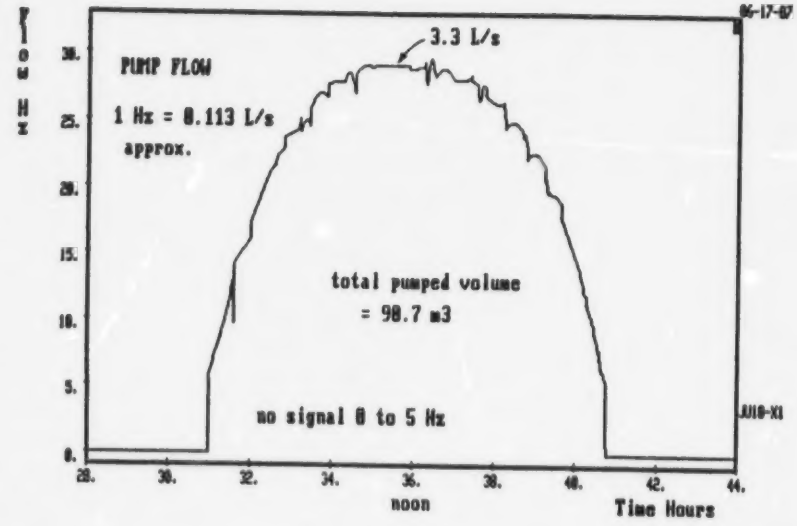


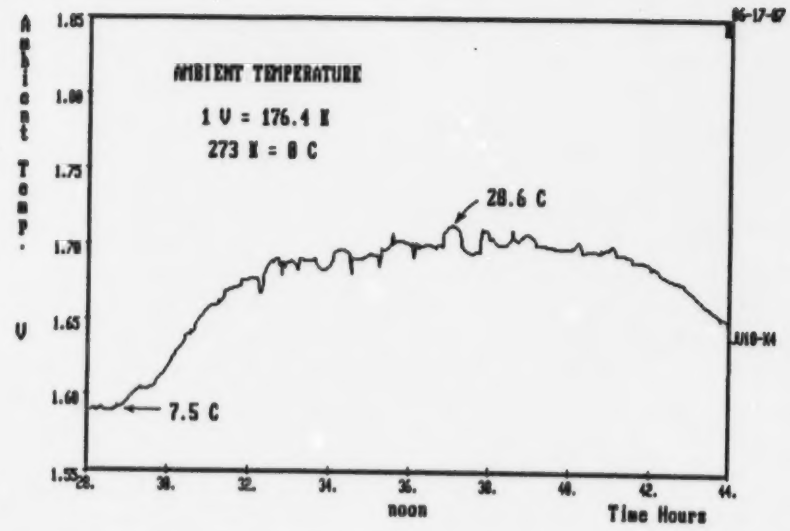


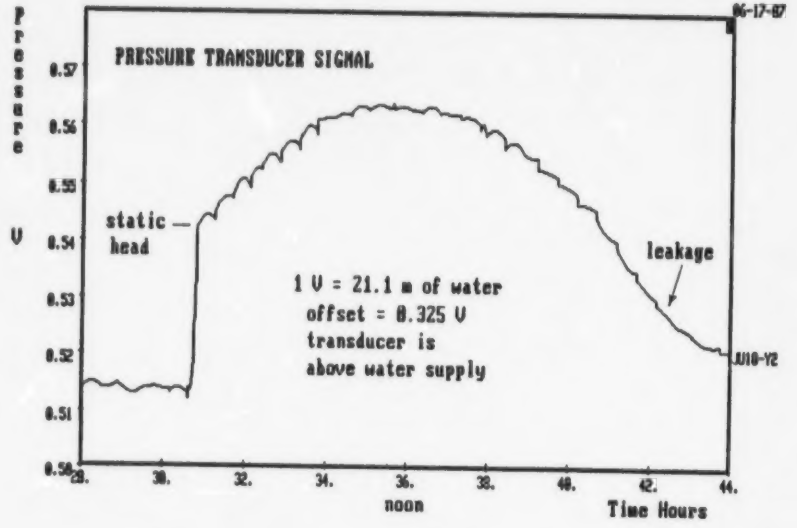


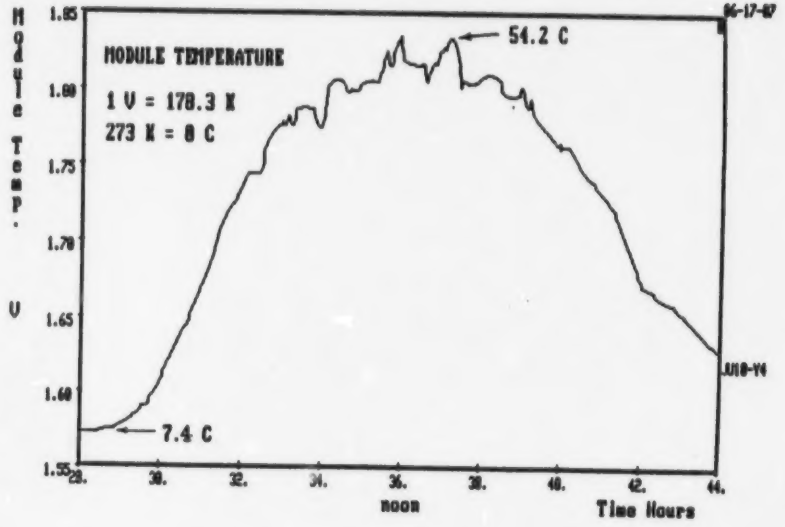


Figure 14. (cont'd) Sample data plots for the pump system in the field on June 17, 1987.

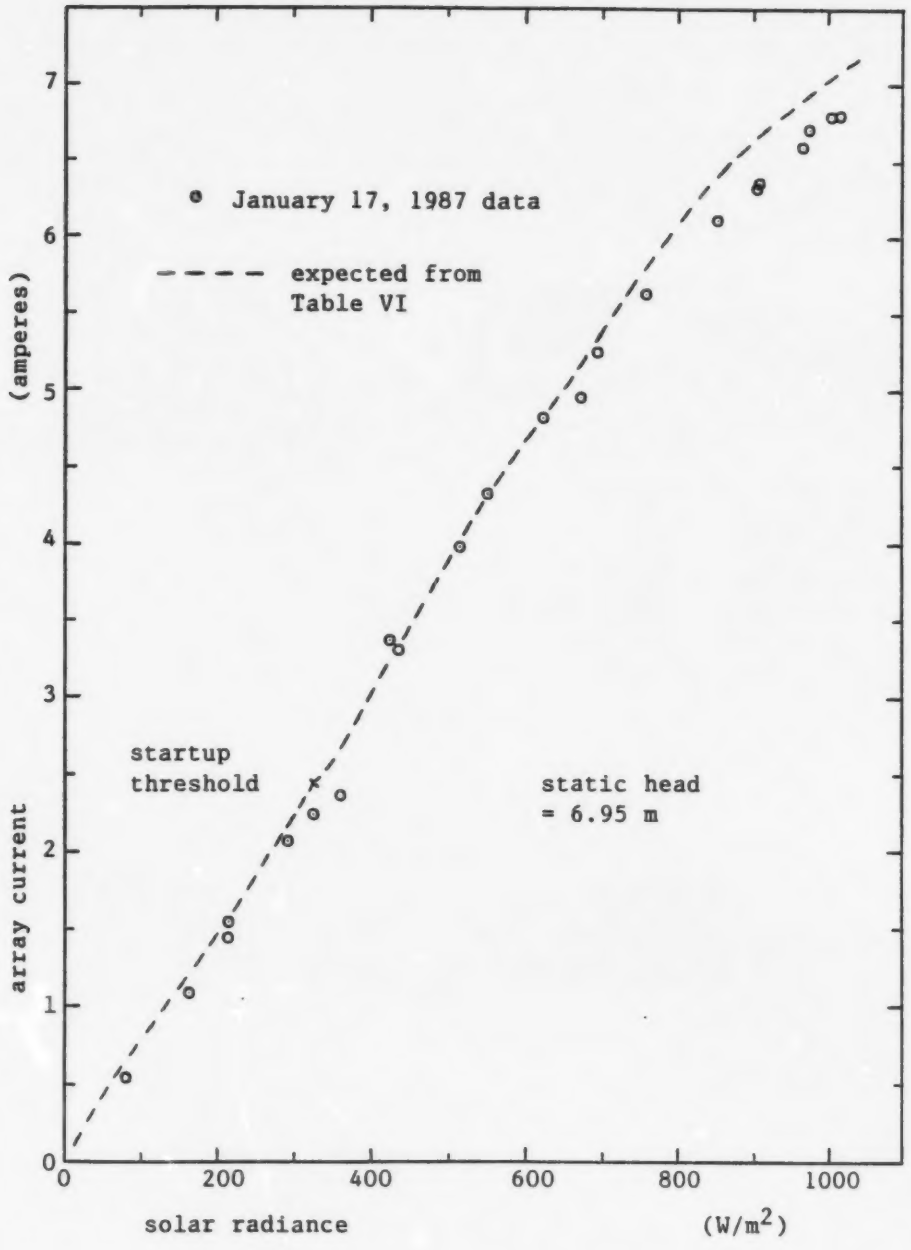


Figure 15. Parametric plot of array current vs irradiance for field data recorded on June 17, 1987.

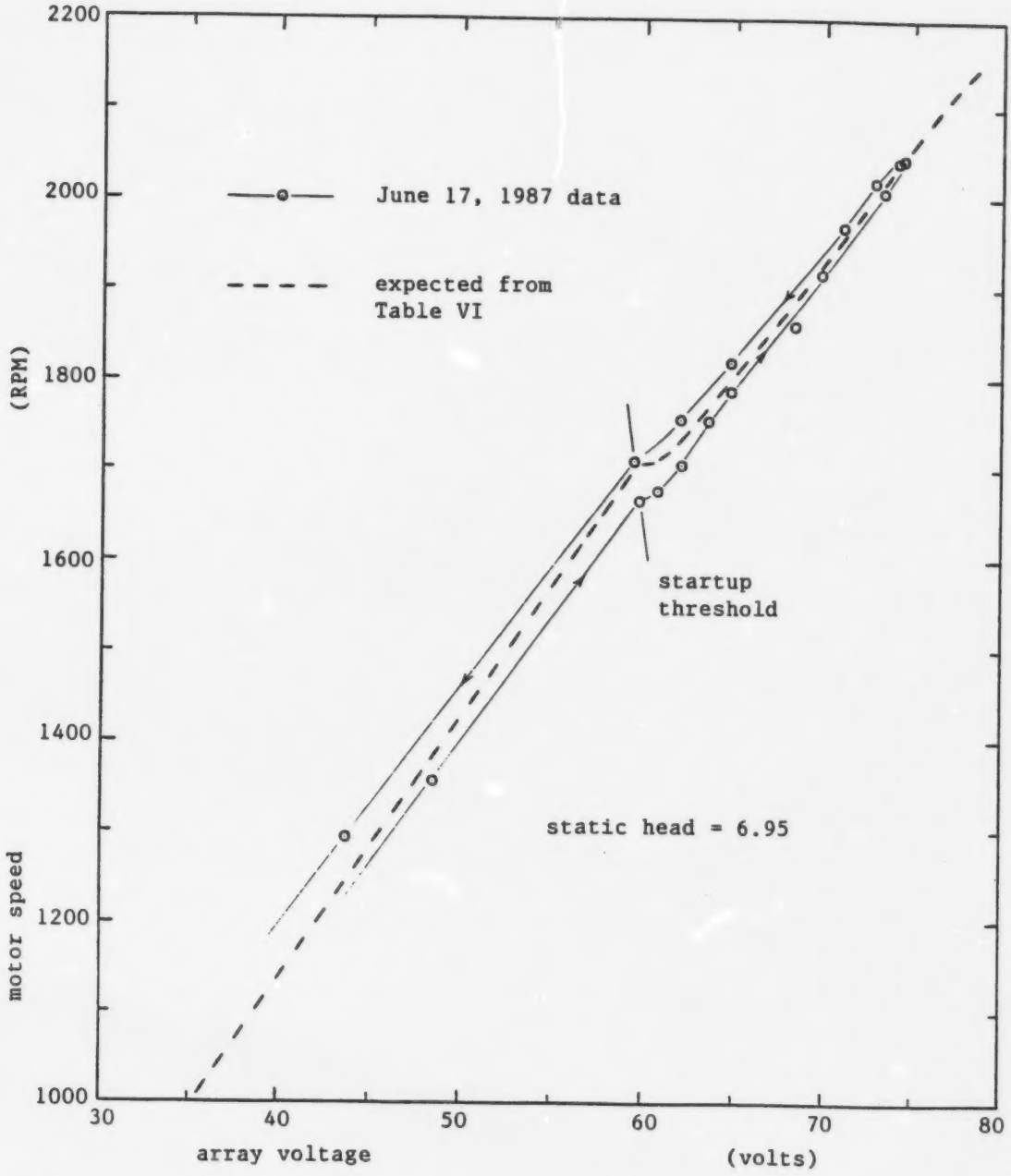


Figure 16. Parametric plot of motor speed versus array voltage for June 17, 1987.

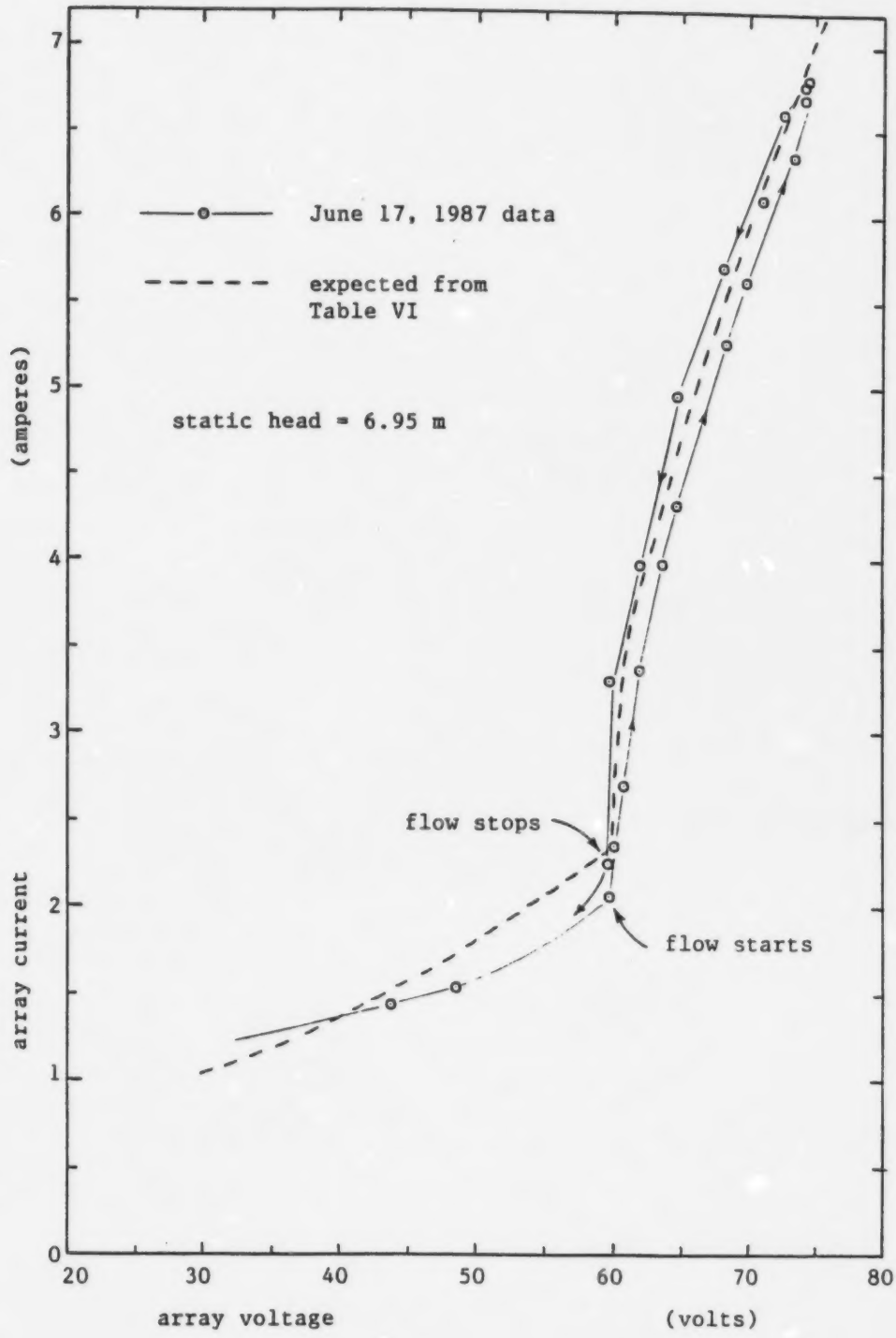


Figure 17. Pump system load line, or parametric plot of current versus voltge for June 17, 1987.

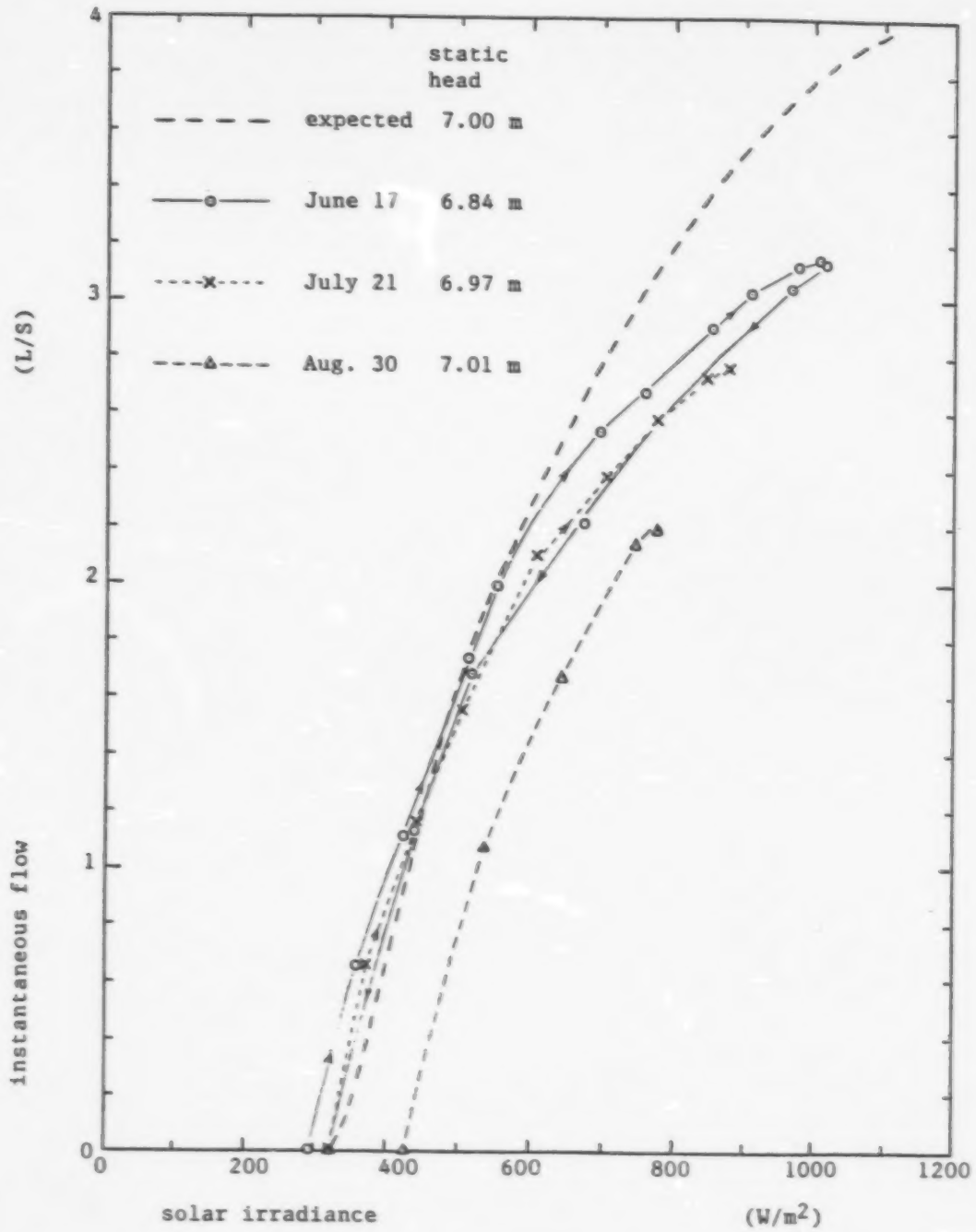


Figure 18. Pump system productivity: parametric plot of flow versus irradiance for three days in 1987.

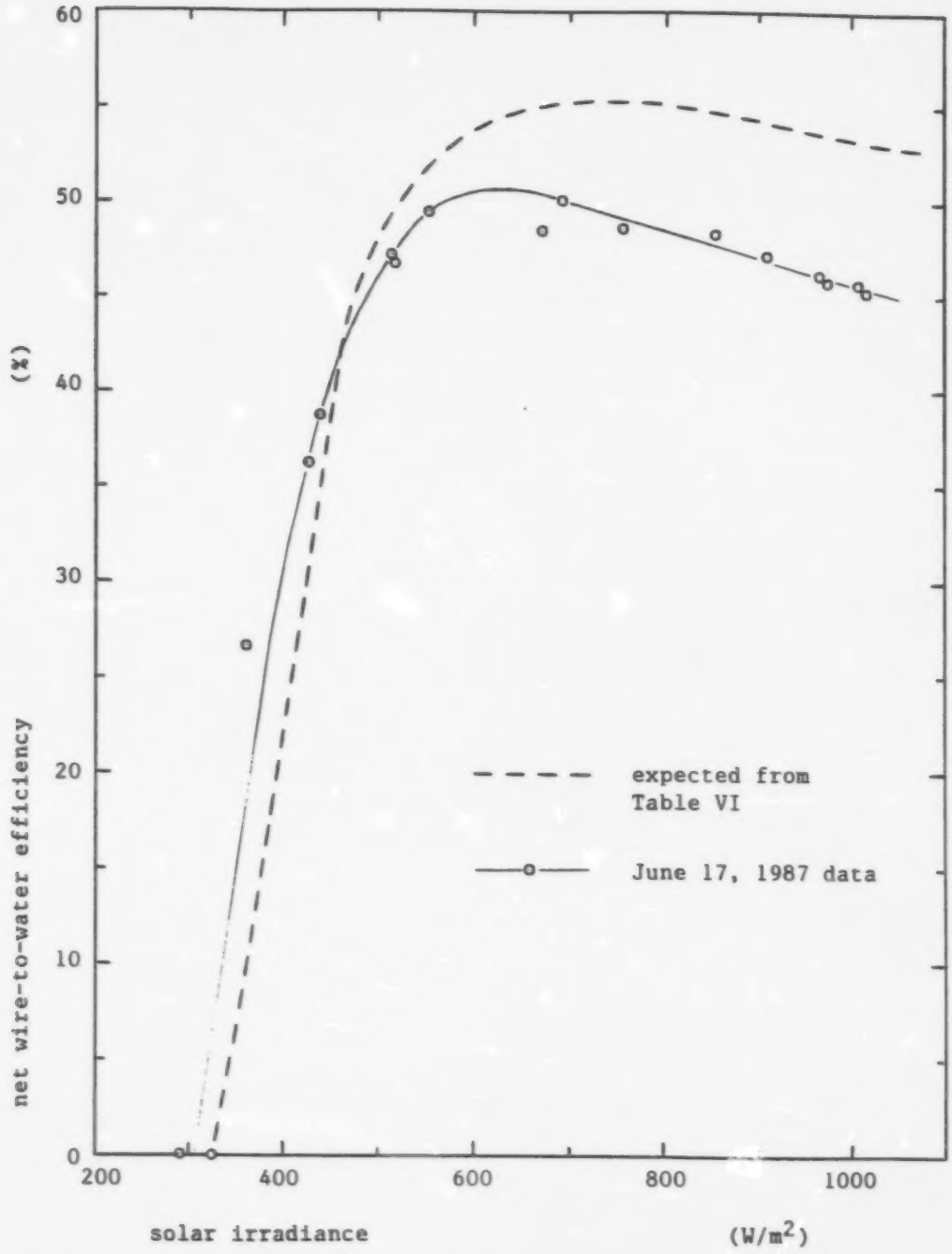


Figure 19. Parametric plot of subsystem efficiency versus irradiance for field data recorded on June 17, 1987.

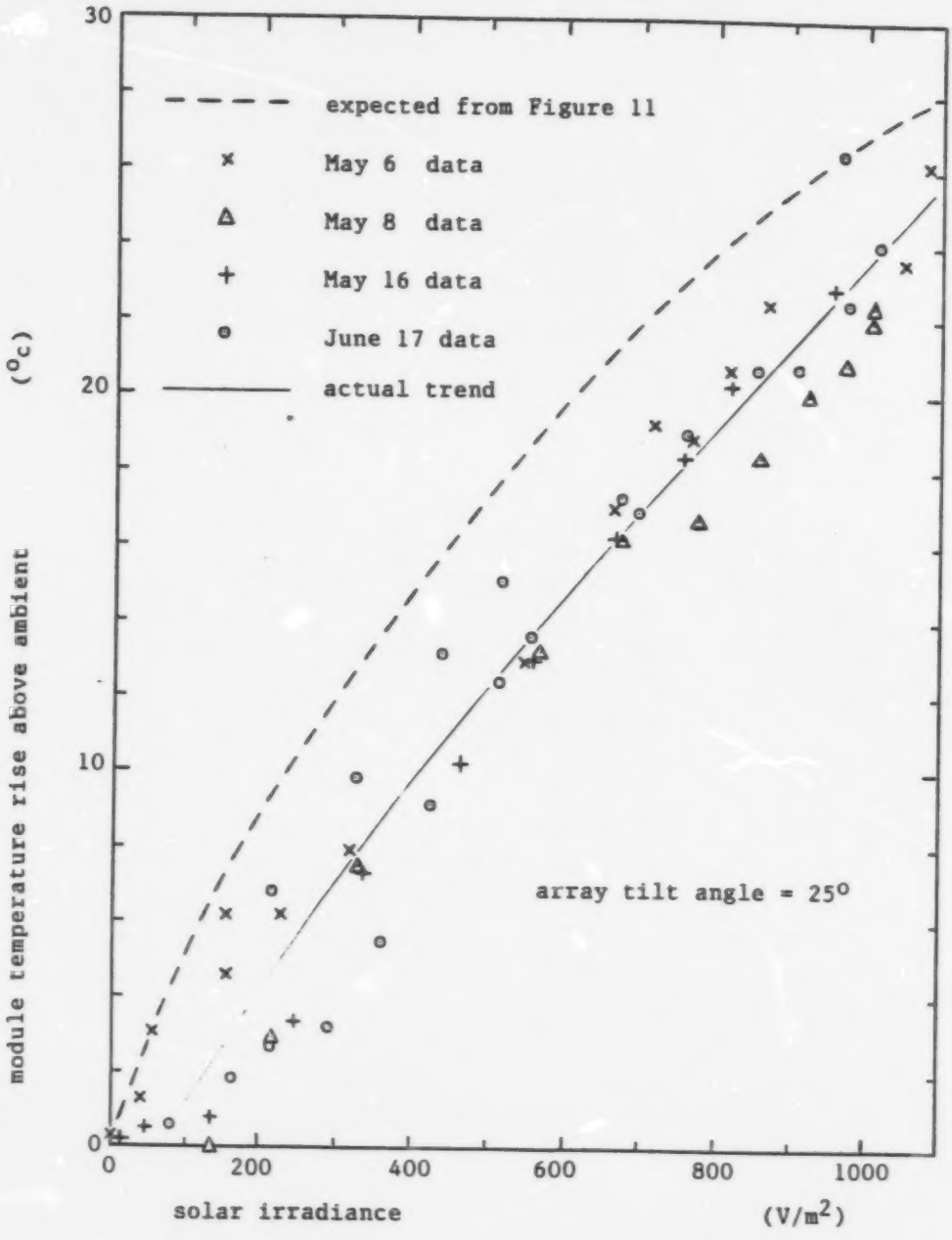


Figure 20. Parametric plot of module heating versus irradiance for clear days in 1987.

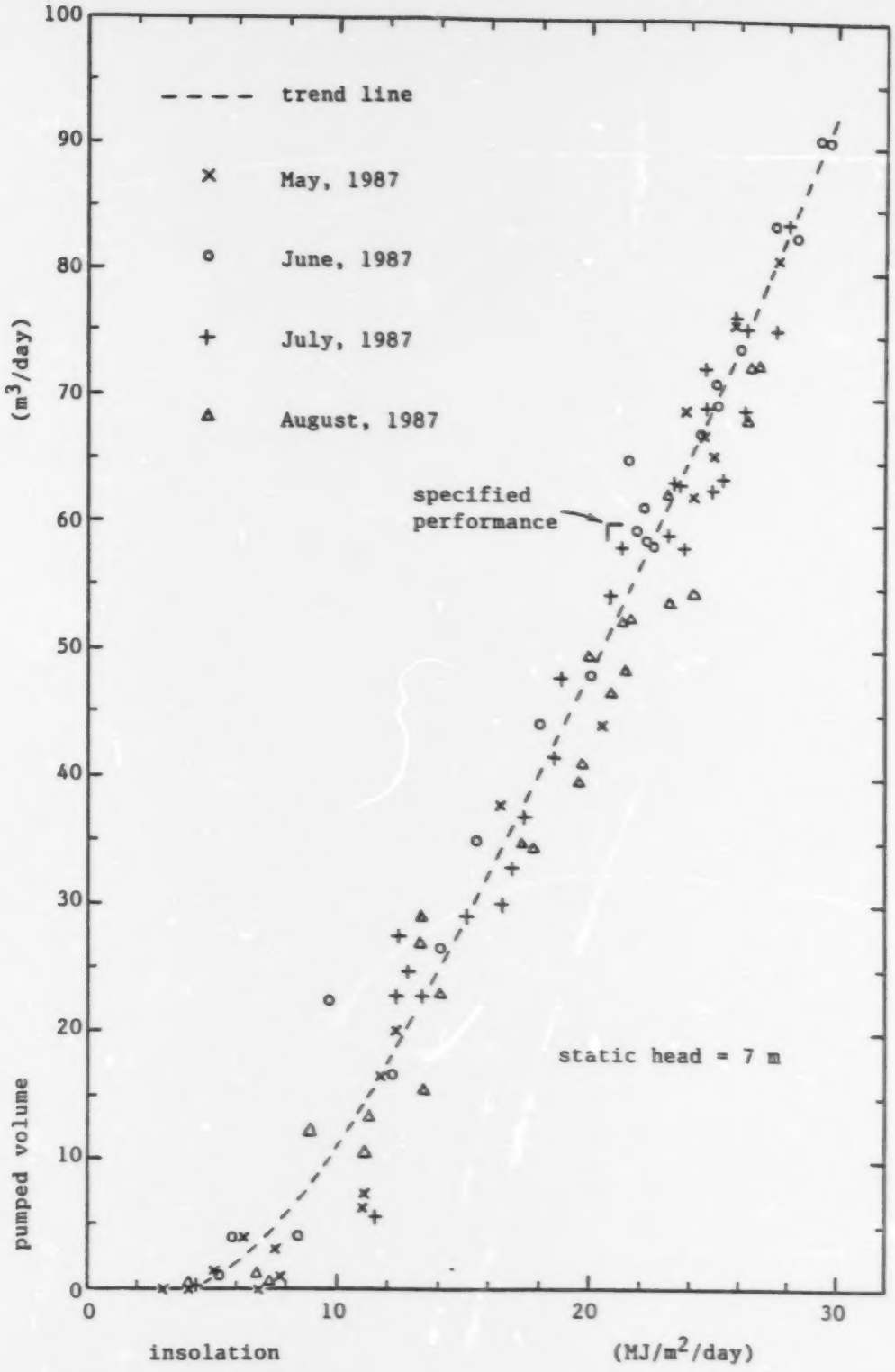


Figure 21. Summary of daily results for four months of PV pump systme field trial.

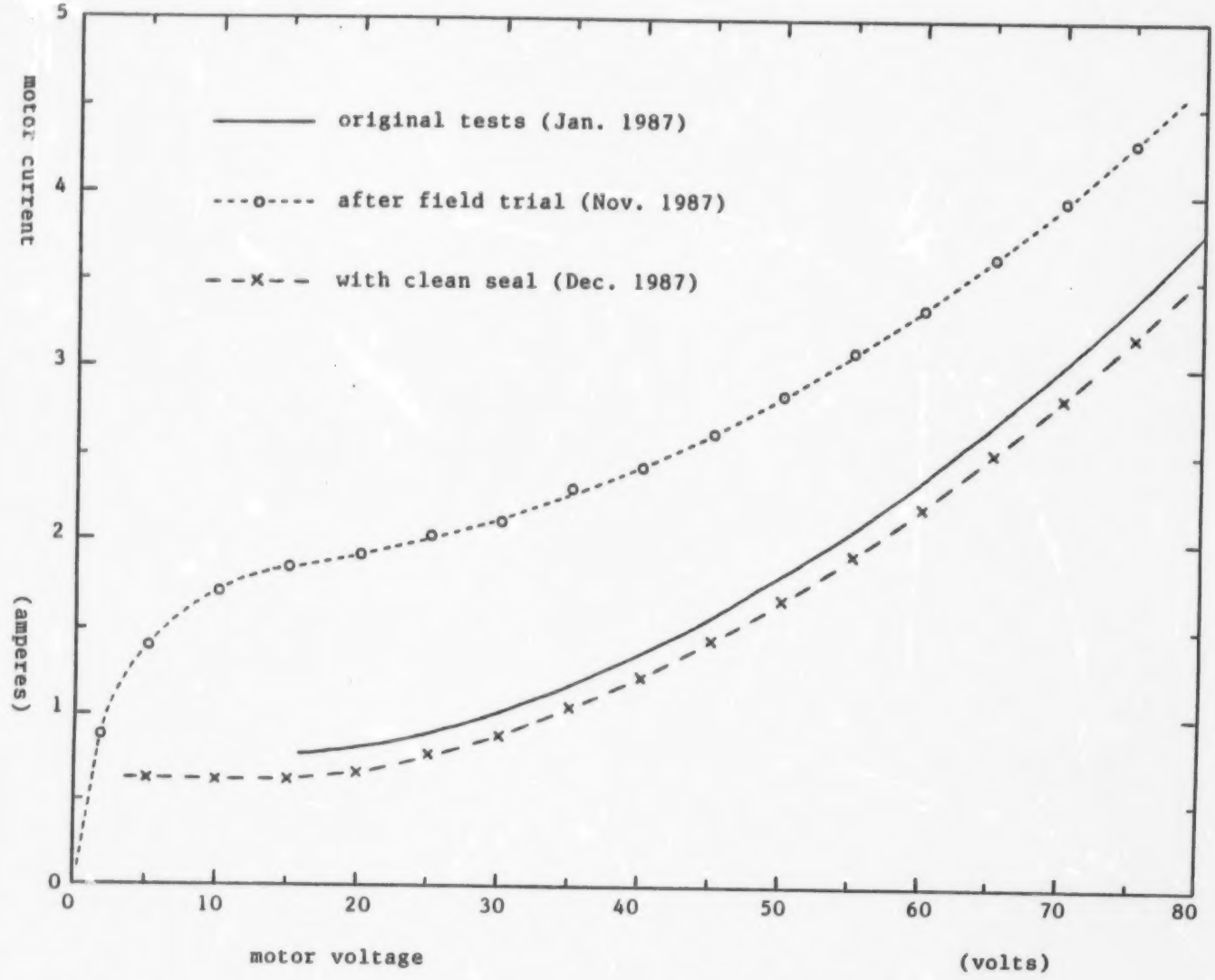


Figure 22. I-V curves for pump/motor subsystem in cutoff (no flow).

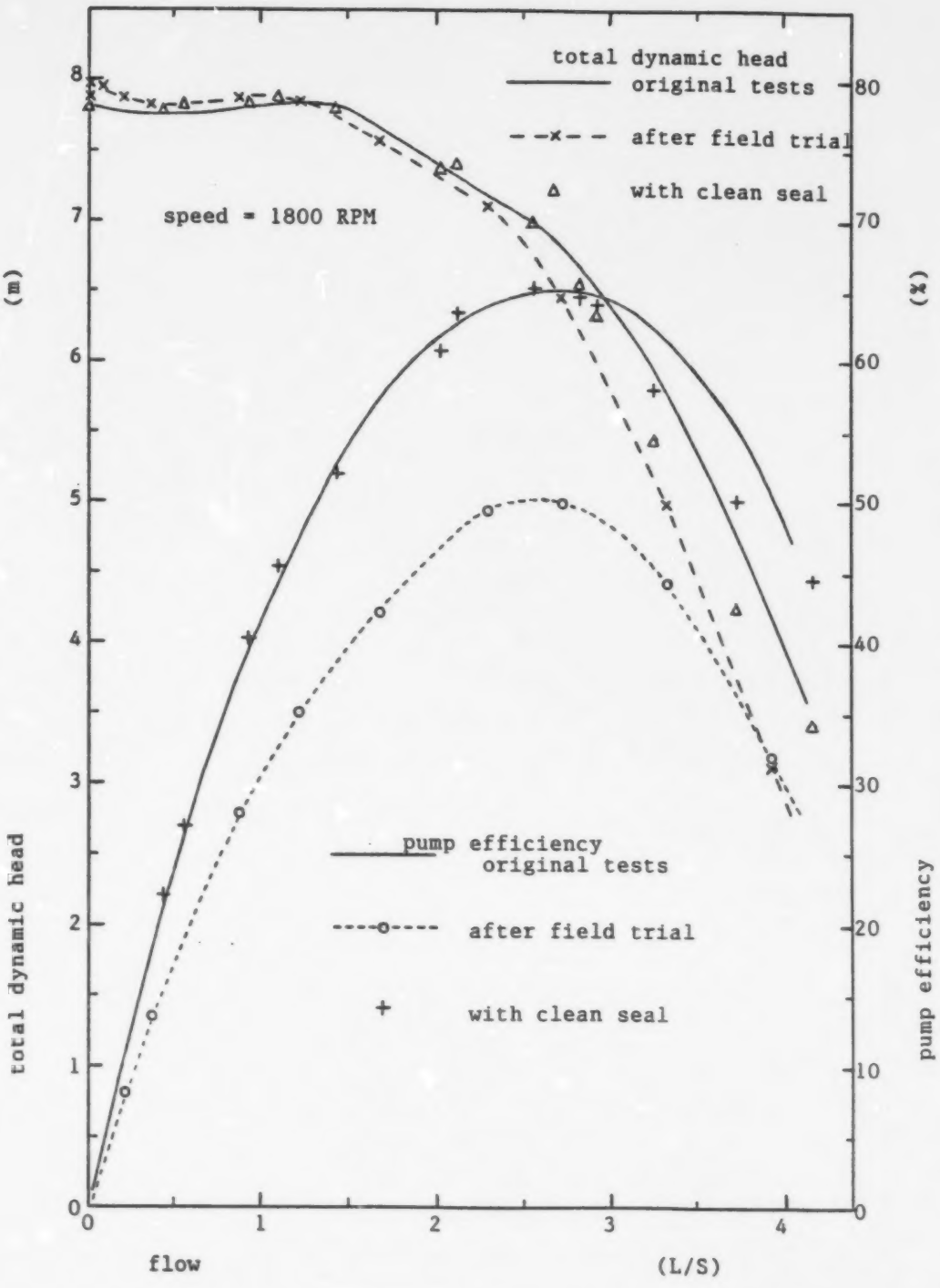


Figure 23. Pump characteristics at 1800 RPM before and after field trial.

| Module Number | Isc (A) | Voc (V) | Pmax (W) | FF (%) |
|---|---|---|---|---|
| 840700701 | 2.25 | 20.6 | 31.1 | 67 |
| " 702 | 2.32 | 20.8 | 30.8 | 64 |
| " 703 | 2.29 | 20.7 | 31.3 | 66 |
| " 704 | 2.17 | 20.6 | 31.2 | 70 |
| " 705 | 2.19 | 20.7 | 30.7 | 68 |
| " 706 | 2.30 | 20.6 | 30.8 | 65 |
| " 707 | 2.29 | 20.7 | 30.9 | 65 |
| " 708 | 2.31 | 20.7 | 30.6 | 64 |
| " 709 | 2.25 | 20.7 | 30.5 | 65 |
| " 710 | 2.26 | 20.8 | 30.8 | 65 |
| " 711 | 2.24 | 20.6 | 30.8 | 67 |
| " 712 | 2.18 | 20.8 | 30.8 | 68 |
| " 713 | 2.26 | 20.6 | 31.4 | 67 |
| " 714 | 2.31 | 20.7 | 31.2 | 65 |
| " 715 | 2.27 | 20.8 | 31.2 | 66 |
| " 716 | 2.26 | 20.8 | 31.3 | 67 |
| " 717 | 2.24 | 20.7 | 31.3 | 67 |
| " 718 | 2.25 | 20.7 | 30.9 | 66 |
| " 719 | 2.23 | 20.7 | 31.0 | 67 |
| " 720 | 2.24 | 20.9 | 30.7 | 65 |
| " 721 | 2.21 | 20.9 | 30.7 | 65 |
| " 722 | 2.26 | 20.8 | 30.9 | 66 |
| " 723 | 2.23 | 20.8 | 31.2 | 67 |
| " 724 | 2.26 | 20.7 | 30.8 | 66 |
| Average value | 2.253 | 20.73 | 30.97 | 66.3 |
| Standard deviation | 0.040 | 0.09 | 0.25 | 1.4 |

Note: Measurements taken under 915 - 1005 $W/m^2$ AM 1.2 sunlight with the solar cells at 19-20°C on May 24, 1984. The values shown are corrected to 1000 $W/m^2$ and 25° cell temperature. $P_{max}$ measured at 16.0 volts. Estimated uncertainty in $P_{max} = \pm 3\%$.

Table I: Measured output for each of the available SW3804 modules at 1000 $W/m^2$ and 25°C.

TABLE II: SIGNAL CALIBRATIONS FOR DATA ACQUISITION SYSTEM.

| CHANNEL | SIGNAL | SIGNAL OFFSET | CONVERSION FACTOR | ESTIMATED UNCERTAINTY | NOTES |
|---|---|---|---|---|---|
| X1 | Flow | N/A | 1 Hz $\approx$ 6.6 Lpm | 2% | erratic below 6 Hz non-linear over active range |
| X2 | Voltage | ~0 | 1 V = 49.4 V | 1% | |
| X3 | Current | + 0.051 V | 1 V = 5.30 A | 1% | |
| X4 | T Ambient | ----- | 1 V = 176.4 K | $\pm$ 1°C | |
| Y1 | Speed | N/A | 1 Hz = 60 RPM | ~0 | |
| Y2 | Pressure | + 0.325 V | 1 V = 21.1 m | 1% | add height to pressure tap |
| Y3 | Sunlight | + 0.042 V | 1 V = 525 W/m$^2$ | 2% relative | standard cell ~40°C |
| Y4 | T Module | ----- | 1 V = 178.3 K | $\pm$ 1°C | |

TABLE III: SAMPLE DATA READINGS FOR MARCH 13, 1987 (SIMULATED STATIC HEAD).

| ME S.T) | X1 FLOW (L/s) | X2 VOLTAGE (volts) | X3 CURRENT (amperes) | X4 T AMBIENT ($^oC$) | Y1 SPEED (RPM) | Y2 PRESSURE (meters) | Y3 SUN ($W/m^2$) | Y4 T MODULE ($^oC$) |
|---|---|---|---|---|---|---|---|---|
| 1:28 | 3.60 | 77.7 | 7.14 | 6.8 | 2106 | 7.69 | 962 | 33.7 |
| 1:47 | 3.59 | 77.9 | 7.23 | 6.9 | 2124 | 7.69 | 975 | 35.3 |
| .2:18 | 3.63 | 78.3 | 7.36 | 8.0 | 2136 | 7.69 | 1000 | 36.4 |
| 12:44 | 3.64 | 78.2 | 7.34 | 3.8 | 2136 | 7.76 | 999 | 33.3 |
| 13:30 | 3.63 | 77.6 | 7.22 | 8.7 | 2124 | 7.69 | 973 | 34.4 |
| 14:16 | 3.51 | 75.5 | 6.84 | 7.5 | 2076 | 7.48 | 898 | 30.3 |
| 14:44 | 3.34 | 72.8 | 6.37 | 7.1 | 2010 | 7.34 | 822 | 28.7 |
| 15:02 | 3.15 | 70.9 | 6.01 | 6.6 | 1962 | 7.23 | 773 | 28.5 |
| 15:15 | 3.05 | 69.3 | 5.72 | 6.1 | 1920 | 7.13 | 728 | 26.2 |
| 15:30 | 2.83 | 67.2 | 5.32 | 6.1 | 1872 | 7.06 | 675 | 23.5 |
| 15:42 | 2.51 | 65.4 | 4.91 | 5.4 | 1824 | 7.06 | 624 | 23.0 |
| 15:54 | 2.30 | 63.7 | 4.55 | 5.5 | 1788 | 6.92 | 579 | 23.5 |
| 16:02 | 2.01 | 62.4 | 4.22 | 5.5 | 1752 | 6.99 | 538 | 22.6 |
| 16:11 | 1.80 | 61.2 | 3.88 | 5.5 | 1728 | 6.92 | 498 | 22.3 |
| 16:20 | 1.42 | 60.3 | 3.52 | 5.0 | 1704 | 6.95 | 455 | 19.8 |
| 16:27 | 1.20 | 59.5 | 3.27 | 5.0 | 1686 | 6.92 | 427 | 19.4 |
| 16:34 | 0.98 | 59.1 | 3.00 | 4.7 | 1692 | 6.92 | 395 | 18.9 |
| 16:38 | 0.77 | 58.8 | 2.83 | 4.8 | 1668 | 6.92 | 376 | 18.7 |
| 16:42 | some | 58.6 | 2.65 | --- | 1686 | 6.92 | 355 | 17.8 |
| 16:48 | 0 (cutoff) | 58.4 | 2.23 | --- | 1680 | 6.90 | 305 | ---- |

TABLE IV: OPERATING RECORD FOR OUTDOOR TESTING NOVEMBER - DECEMBER, 1986

| DATE 1986 | WEATHER | DATA ACQUISITION STATUS | HOURS LOGGED | INSOLATION | PUMPED VOLUME | COMMENTS/NOTES |
|---|---|---|---|---|---|---|
| Nov. 21 | cloudy/snow | installation | 0 | ---- | ---- | setting up system |
| 22 | sunny breaks | 6 of 8 channels working | ? | ? | some | pump system operating |
| 23 | ? | partial recording | ? | ? | ? | |
| Mon. 24 | ? | partial recording | ? | ? | ? | |
| 25 | sunny breaks | down for debugging | ? | ? | some | experiments with loggers |
| 26 | cloudy | partial recording | ? | ? | 0 | |
| 27 | sunny | partial recording | ? | ? | some | debugging noisy signals |
| Fri. 28 | sunny periods | partial recording | ? | ? | some | debugging noisy signals |
| 29 | sunny breaks | recording | ? | ? | some | |
| Nov. 30 | sunny breaks | recording | ? | ? | some | |
| Dec. 01 | clear & sunny | calibrating sensors | ? | ---- | ---- | pyranometer replaced |
| 02 | cloudy/snow | data playback | ~0 | ? | 0 | debugging speed sensor |
| 03 | cloudy/dull | all channels working | ~4 | ? | 0 | noise problems solved |
| 04 | sunny breaks | recording | 7 | 3.9 | ~0.5 $m^3$ | some glitches in data |
| Fri. 05 | scattered clouds | " | 20 | 18.3 $MJ/m^2$ | 46.5 $m^3$ | |
| 06 | sunny breaks | " | 24 | 2.0 | 0 | |
| 07 | sunny breaks/snow | " | 19 | 2.4 | 0 | |
| Mon. 08 | clear & cold | good data | 8 | 19.3 $MJ/m^2$ | 56.9 $m^3$ | best data |
| 09 | overcast/snow | " | 9 | 0.8 | 0 | |
| 10 | snow/clearing | " | 9 | 5.7 | 15.0 $m^3$ | |
| 11 | cloudy periods | " | 9 | 8.7 | 17.1 $m^3$ | |
| Fri. 12 | snow/clearing | " | 9 | 13.6 | 23.3 $m^3$ | some glitches in data |
| 13 | clear & cold | recording | 24 | 20.4 | 36.6 | pump losing prime |
| 14 | cloudy | " | 24 | 3.1 | 0 | |
| Dec. 15 | ? | shut down | 0 | ---- | ---- | dismantle pump subsystem |

**TABLE V:** Sample data listings at ten minute intervals for two channels from the data loggers, recorded on December 8, 1986.

DC8-X1.LOG

Sensor type 25 (Counting ( < 1Khz)).

| Calendar | Value | Average | Max | Min |
|---|---|---|---|---|
| 8: 8:31: 1 | 0.0000 | 0.0000 | 0.0000 | 0.0000 |
| 8: 8:41: 1 | 0.0000 | 0.0000 | 0.0000 | 0.0000 |
| 8: 8:51: 1 | 0.0000 | 0.0000 | 0.0000 | 0.0000 |
| 8: 9: 1: 1 | 0.0000 | 0.0000 | 0.0000 | 0.0000 |
| 8: 9:11: 1 | 0.0000 | 0.0000 | 0.0000 | 0.0000 |
| 8: 9:21: 1 | 10.0071 | 3.6507 | 21.5000 | 0.0000 |
| 8: 9:31: 1 | 11.4078 | 10.7509 | 21.5000 | 4.9000 |
| 8: 9:41: 1 | 13.5937 | 11.4040 | 14.4000 | 0.9000 |
| 8: 9:51: 1 | 14.8331 | 14.0928 | 16.4000 | 9.8000 |
| 8:10: 1: 1 | 15.0646 | 14.9320 | 16.5000 | 12.9000 |
| 8:10:11: 1 | 20.2722 | 17.9422 | 22.8000 | 13.9000 |
| 8:10:21: 1 | 20.7825 | 20.7970 | 23 | 18.2000 |
| 8:10:31: 1 | 23.3276 | 22.1569 | 25.7000 | 19.4000 |
| 8:10:41: 1 | 26.0808 | 24.7655 | 28.7000 | 21.6000 |
| 8:10:51: 1 | 26.8532 | 26.4552 | 30 | 24 |
| 8:11: 1: 1 | 28.5200 | 27.6540 | 29.4000 | 24.2000 |
| 8:11:11: 1 | 30.2204 | 28.8199 | 31.2027 | 26.4000 |
| 8:11:21: 1 | 29.2794 | 30.4858 | 32.1000 | 28.3000 |
| 8:11:31: 1 | 30.3534 | 30.3760 | 33 | 28 |
| 8:11:41: 1 | 33.2180 | 32.5365 | 34.2407 | 28.9000 |
| 8:11:51: 1 | 33.5391 | 33.4833 | 35.3000 | 32.1000 |
| 8:12: 1: 1 | 34.5700 | 34.0292 | 35.9000 | 32.1000 |
| 8:12:11: 1 | 34.7851 | 35.0184 | 37.7000 | 33 |
| 8:12:21: 1 | 34.9469 | 35.2537 | 37.9000 | 33.9000 |
| 8:12:31: 1 | 35.0477 | 35.1116 | 37.9000 | 33.8000 |
| 8:12:41: 1 | 33.9678 | 34.4267 | 36.6000 | 27.3000 |
| 8:12:51: 1 | 34.5970 | 31.4134 | 36.9000 | 11.6000 |

DC8-Y3.LOG

Sensor type 13 (Voltage).

| Calendar | Value | Average | Max | Min |
|---|---|---|---|---|
| 8: 8:31: 7 | 0.8511 | 0.7970 | 0.8566 | 0.7410 |
| 8: 8:41: 7 | 0.9534 | 0.9023 | 0.9630 | 0.8456 |
| 8: 8:51: 7 | 1.0504 | 1.0012 | 1.0571 | 0.9490 |
| 8: 9: 1: 7 | 1.1400 | 1.0959 | 1.1472 | 1.0461 |
| 8: 9:11: 7 | 1.2209 | 1.1794 | 1.2264 | 1.1332 |
| 8: 9:21: 7 | 1.3070 | 1.2635 | 1.3186 | 1.2170 |
| 8: 9:31: 7 | 1.3830 | 1.3462 | 1.3914 | 1.3006 |
| 8: 9:41: 7 | 1.4569 | 1.4214 | 1.4664 | 1.3780 |
| 8: 9:51: 7 | 1.5255 | 1.4932 | 1.5343 | 1.4514 |
| 8:10: 1: 7 | 1.5911 | 1.5583 | 1.5960 | 1.5133 |
| 8:10:11: 7 | 1.6456 | 1.6210 | 1.6551 | 1.5848 |
| 8:10:21: 7 | 1.7028 | 1.6742 | 1.7103 | 1.6401 |
| 8:10:31: 7 | 1.7481 | 1.7239 | 1.7550 | 1.6963 |
| 8:10:41: 7 | 1.7850 | 1.7670 | 1.7970 | 1.7380 |
| 8:10:51: 7 | 1.8300 | 1.8089 | 1.8382 | 1.7760 |
| 8:11: 1: 7 | 1.8656 | 1.8495 | 1.8781 | 1.8232 |
| 8:11:11: 7 | 1.8979 | 1.8823 | 1.9047 | 1.8531 |
| 8:11:21: 7 | 1.9177 | 1.9088 | 1.9230 | 1.8917 |
| 8:11:31: 7 | 1.9392 | 1.9334 | 1.9490 | 1.9110 |
| 8:11:41: 7 | 1.9508 | 1.9442 | 1.9630 | 1.9300 |
| 8:11:51: 7 | 1.9689 | 1.9624 | 1.9797 | 1.9360 |
| 8:12: 1: 7 | 1.9734 | 1.9725 | 1.9880 | 1.9480 |
| 8:12:11: 7 | 1.9797 | 1.9782 | 1.9920 | 1.9630 |
| 8:12:21: 7 | 1.9713 | 1.9841 | 1.9960 | 1.9460 |
| 8:12:31: 7 | 1.9700 | 1.9782 | 1.9950 | 1.9460 |
| 8:12:41: 7 | 1.9018 | 1.9471 | 1.9810 | 1.7604 |
| 8:12:51: 7 | 1.9439 | 1.8067 | 1.9730 | 1.0850 |

TABLE VI: CALCULATED OPERATING POINTS FOR THE PUMP SYSTEM IN STEADY-STATE OPERATION AT 7.0 m STATIC HEAD AND 25°C AMBIENT.

| PARAMETER | | SELECTED OPERATING POINTS | | | | | | | | | | UNITS |
|---|---|---|---|---|---|---|---|---|---|---|---|---|
| Q | flow | 4.105 | 3.80 | 3.55 | 2.78 | 2.16 | 1.49 | 0.913 | 0.39 | 0.18 | 0.00 | L/s |
| TDH | total dynamic head | 7.79 | 7.67 | 7.59 | 7.34 | 7.23 | 7.10 | 7.05 | 7.02 | 7.00 | 7.00 | m |
| $\eta_p$ | pump efficiency | 60.0 | 62.0 | 63.0 | 65.0 | 63.0 | 55.0 | 40.0 | 20.0 | 10.0 | 0.0 | % |
| S | shaft speed | 2149 | 2074 | 2014 | 1864 | 1791 | 1720 | 1703 | 1709 | 1709 | 1704 | RPM |
| Phyd. | hydraulic power | 313 | 286 | 264 | 200 | 153 | 104 | 63.1 | 26.8 | 12.3 | 0.0 | W |
| Pmech. | shaft power | 522 | 461 | 419 | 308 | 243 | 189 | 158 | 134 | 124 | ~114 | W |
| $\tau$ | torque | 2.32 | 2.12 | 1.99 | 1.58 | 1.30 | 1.05 | 0.88 | 0.75 | 0.69 | 0.64 | Nm |
| V | voltage | 78.5 | 75.2 | 73.1 | 67.3 | 64.2 | 61.2 | 60.2 | 60.2 | 60.0 | 59.7 | V |
| I | current | 7.70 | 7.09 | 6.69 | 5.39 | 4.50 | 3.70 | 3.26 | 2.80 | 2.60 | 2.45 | A |
| Pelect. | electric power | 605 | 536 | 489 | 361 | 288 | 227 | 196 | 168 | 156 | ~146 | W |
| $\eta_m$ | motor efficiency | 86 | 86 | 86 | 85.2 | 84.3 | 82.9 | 81 | 80 | 79 | 78 | % |
| Psun | solar irradiance | ~1300 | 1016 | 912 | 701 | 582 | 480 | 427 | 377 | 353 | 324 | $W/m^2$ |
| $\eta_{w-w}$ | subsystem efficiency | 51.6 | 53.3 | 54.2 | 55.4 | 53.1 | 45.6 | 32.6 | 16.0 | 7.9 | 0.0 | % |

Table VII. Summary of field trial results for the month of May.

| date (1987) | recorded signals (No.) | (hrs) | static head (m) | insol-ation (MJ/m²) | pump time (hours) | volume pumped (m³) | events and notes |
|---|---|---|---|---|---|---|---|
| May 1-4 | 0 | 0 | - | ? | [0] | [0] | setting up, pump off |
| May 5 | 7 | [8.2] | 6.75 | [1.3] | [0.4] | [2.0] | finish setup, note 1 |
| May 6 | 7 | 21.8 | ~6.80 | 23.8 | 8.1 | 69.1 | note 2 |
| May 7 | 8 | L[10.5] | 6.86 | [5.7] | [2.9] | [21.0] | calibrate sensors, 1 |
| May 8 | 8 | 24 | ~6.86 | 24.9 | 9.9 | 65.5 | |
| May 9 | 8 | 24 | ~6.86 | 20.5 | 6.2 | 44.1 | |
| May 10 | 8 | 24 | ~6.87 | [21.9] | 9.1 | 77.5 | notes 2,3 |
| May 11 | 8 | 18.2 L | 6.87 | 5.1 | 1.6 | 1.4 | |
| May 12 | 8 | 24 | ~6.90 | [28.5] | 9.4 | 67.5 | note 3 |
| May 13 | 8 | 24 | ~6.92 | [23.4] | 9.4 | 85.1 | notes 2,3 |
| May 14 | 8 | 24 | ~6.95 | 24.6 | [7.3] | [67.0] | note 4 |
| May 15 | 8 | 19.2 L | 6.97 | 25.8 | 9.3 | 75.7 | |
| May 16 | 8 | 14.4 L | ~7.00 | 16.4 | 5.3 | 37.8 | |
| May 17 | 8 | 15.0 L | ~7.03 | 4.2 | 0 | 0 | no pumping |
| May 18 | 8 | 14.6 L | 7.05 | 11.0 | 2.0 | 6.3 | |
| May 19 | 8 | 17.3 L | ~7.08 | 27.6 | 9.0 | 81.1 | |
| May 20 | 3 | 24 | ~7.10 | 11.1 | 2.3 | 7.3 | |
| May 21 | 3 | 24 | ~7.12 | 12.4 | 5.2 | 20.0 | |
| May 22 | 3 | 24 | ~7.15 | 6.4 | 1.4 | 4.0 | |
| May 23 | 3 | 24 | ~7.16 | 3.1 | 0 | 0 | no pumping |
| May 24 | 3 | 24 | ~7.17 | 7.0 | 0 | 0 | no pumping |
| May 25 | 3 | ~18.5 L | 7.18 | 24.1 | 9.8 | 62.1 | rearrange discharge |
| May 26 | 3 | 24 | ~7.20 | 11.8 | 4.0 | 16.6 | |
| May 27 | 3 | 24 | ~7.15 | 7.6 | 1.2 | 3.2 | |
| May 28 | 3 | 24 | ~7.10 | 16.4 | [3.0] | [24.4] | note 4 |
| May 29 | 3 | 17.0 L | 7.09 | 22.2 | [6.2] | [45.4] | note 4 |
| May 30 | 3 | 24 | ~7.12 | 21.7 | [7.4] | [41.8] | notes 4,5 |
| May 31 | 3 | 24 | ~7.15 | 7.8 | 1.7 | 1.0 | note 5 |
| totals: | (18 days) | | - | 250.6 | 77.0 | 495.2 | |
| averages: | - | | 7.05 | 13.9 | 4.28 | 27.5 | avg. flow = 1.79 L/s |

notes: - "L" means data logged before or after recording period.
- ~ static head means interpolated between measured values.
- [x] means value incorrect , anomalous or suspect.

1: data logged for only part of total operating period.
2: pressure signal glitch (goes offscale and then to zero).
3: data compaction in indicated signal; data unreliable.
4: flow starts late, at too high a voltage; volume too low.
5: irradiance signal conditioning problem; signal corrected.

Table VIII. Summary of field trial results for the month of June.

| date (1987) | recorded signals (No.) | (hrs) | static head (m) | insol-ation (MJ/m²) | pump time (hours) | volume pumped (m³) | events and notes |
|---|---|---|---|---|---|---|---|
| Jun. 1 | 3 | 24 | ~7.18 | 20.0 | 9.0 | 48.0 | note 5 |
| Jun. 2 | 3 | 24 | ~7.20 | 22.5 | 8.3 | 58.3 | note 5 |
| Jun. 3 | 3 | 24 | ~7.22 | 5.2 | 0.5 | 1.3 | note 5 |
| Jun. 4 | 3 | 24 | ~7.24 | 22.3 | 9.5 | 58.6 | note 5 |
| Jun. 5 | 3 | 16.8 L | 7.25 | 14.0 | 6.5 | 26.5 | adjust discharge, 5 |
| Jun. 6 | 3 | 13.6 L | 7.00 | ~28.4 | 9.7 | 82.9 | check/clean sensors,5 |
| Jun. 7 | 3 | 24 | ~6.98 | 5.8 | 1.4 | 4.0 | note 5 |
| Jun. 8 | 3 | 24 | ~6.96 | 9.6 | 4.2 | 22.4 | note 5 |
| Jun. 9 | 3 | 24 | ~6.94 | 7.1 | [?] | [19.4] | notes 3,5 |
| Jun.10 | 3 | 24 | ~6.92 | 28.6 | 9.5 | [71.1] | notes 3,5 |
| Jun.11 | 3 | 24 | ~6.90 | 21.5 | 7.9 | 65.0 | note 5 |
| Jun.12 | 3 | 24 | ~6.90 | 8.4 | 1.9 | 4.2 | note 5 |
| Jun.13 | 3 | 24 | ~6.88 | 18.0 | 8.5 | 44.0 | note 5 |
| Jun.14 | 3 | 24 | ~6.86 | 21.9 | 8.7 | 59.3 | note 5 |
| Jun.15 | 3 | 24 | ~6.84 | 28.1 | [8.5] | [75.2] | notes 4,5 |
| Jun.16 | 3 | 18.2 L | 6.82 | 15.5 | 5.8 | 34.8 | note 5 |
| Jun.17 | 8 | 24 | ~6.84 | 29.3 | 9.8 | 90.7 | best day, note 5 |
| Jun.18 | 8 | 17.5 L | 6.86 | 27.5 | 9.5 | 83.8 | note 5 |
| Jun.19 | 8 | 24 | ~6.86 | 22.2 | 7.4 | 61.4 | |
| Jun.20 | 8 | 24 | ~6.87 | 29.7 | 8.8 | 90.5 | |
| Jun.21 | 8 | 24 | ~6.88 | 24.5 | 8.0 | 67.1 | |
| Jun.22 | 8 | 24 | ~6.88 | 12.1 | 3.5 | 16.8 | |
| Jun.23 | 8 | 17.0 L | 6.89 | 25.0 | 7.5 | 71.1 | |
| Jun.24 | 3 | 24 | ~6.90 | 26.1 | 9.3 | 74.0 | |
| Jun.25 | 3 | ~17 | ~6.91 | 25.2 | 9.1 | 69.5 | extend suction pipe |
| Jun.26 | 0 | 0 | ~6.91 | ? | [0] | [0] | prime pump, no data |
| Jun.27 | 3 | 24 | ~6.93 | 15.5 | [0] | [0] | lost prime, note 5 |
| Jun.28 | 3 | 24 | ~6.94 | 17.9 | [0] | [0] | no pumping, note 5 |
| Jun.29 | 3 | 24 | ~6.95 | 5.7 | [0] | [0] | no pumping, note 5 |
| Jun.30 | 3 | 24 | ~6.96 | 24.6 | [0] | [0] | find leak, pump off, 5 |
| totals: (22 days) | | - | | 434.7 | 154.8 | 1134.2 | |
| averages: | | - | 6.97 | 19.8 | 7.04 | 51.6 | avg. flow = 2.03 L/s |

notes: - "L" means data logged before or after recording period.
- ~ static head means interpolated between measured values.
- [x] means value incorrect , anomalous or suspect.
3: data compaction in indicated signal; data unreliable.
4: flow starts late, at too high a voltage; volume too low.
5: irradiance signal conditioning problem; signal corrected.

Table IX. Summary of field trial results for the month of July.

| date (1987) | recorded signals (No.) | (hrs) | static head (m) | insol-ation (MJ/m²) | pump time (hours) | volume pumped (m³) | events and notes |
|---|---|---|---|---|---|---|---|
| Jul. 1 | 3 | 24 | ~6.97 | 21.0 | [0] | [0] | holiday, pump off, 5 |
| Jul. 2 | 3 | ~17 L | 6.99 | 15.0 | [0] | [0] | fix leak & prime, 5 |
| Jul. 3 | 8 | 24 | ~6.99 | 11.5 | 1.6 | 5.6 | |
| Jul. 4 | 8 | 24 | ~6.99 | 18.6 | 9.1 | 41.4 | |
| Jul. 5 | 8 | 24 | ~6.98 | 28.0 | 9.8 | 83.9 | |
| Jul. 6 | 8 | 24 | ~6.98 | 24.6 | 9.2 | 69.2 | |
| Jul. 7 | 8 | 16.7 L | 6.98 | 12.4 | 5.8 | 27.5 | |
| Jul. 8 | 3 | 24 | ~6.98 | 15.1 | 4.9 | 29.1 | |
| Jul. 9 | 3 | 24 | ~6.97 | 26.2 | 7.8 | 69.0 | |
| Jul.10 | 3 | 24 | ~6.97 | 16.5 | 6.5 | 30.0 | |
| Jul.11 | 3 | 24 | ~6.96 | 16.9 | 7.0 | 32.8 | |
| Jul.12 | 3 | 24 | ~6.96 | 21.2 | 7.5 | 58.1 | |
| Jul.13 | 3 | 24 | ~6.95 | 17.4 | 6.8 | 36.9 | |
| Jul.14 | 3 | 24 | ~6.95 | 4.4 | 0.3 | 0.3 | |
| Jul.15 | 3 | L[14.9] | 6.94 | [22.2] | [8.1] | [68.8] | note 1 |
| Jul.16 | 3 | 24 | ~6.94 | 25.3 | 8.4 | 63.6 | |
| Jul.17 | 3 | 24 | ~6.95 | 23.6 | 8.2 | 63.1 | |
| Jul.18 | 3 | 24 | ~6.95 | 18.9 | 8.6 | 47.8 | |
| Jul.19 | 3 | 24 | ~6.96 | 12.3 | 5.0 | 22.8 | |
| Jul.20 | 3 | 24 | ~6.96 | 13.3 | 7.0 | 22.8 | |
| Jul.21 | 3 | 24 | ~6.97 | 26.3 | 9.2 | 75.6 | |
| Jul.22 | 3 | 24 | ~6.97 | 24.9 | 9.2 | 62.3 | |
| Jul.23 | 3 | 17.3 L | 6.98 | 22.4 | [6.8] | [38.7] | note 6 |
| Jul.24 | 3 | 24 | ~6.98 | 12.8 | 5.7 | 24.7 | |
| Jul.25 | 3 | 24 | ~6.99 | 20.8 | 8.0 | 54.2 | |
| Jul.26 | 3 | 24 | ~6.99 | 24.6 | 9.6 | 72.4 | |
| Jul.27 | 3 | 24 | ~7.00 | 25.9 | 9.5 | 76.4 | |
| Jul.28 | 3 | 24 | ~7.00 | 23.4 | 9.2 | 63.2 | |
| Jul.29 | 3 | 24 | ~7.00 | 23.8 | 8.7 | 58.1 | |
| Jul.30 | 3 | 17.2 L | 7.00 | 23.2 | 9.2 | 59.1 | |
| Jul.31 | 3 | 24 | ~7.00 | 27.5 | 8.7 | 75.3 | |
| totals: | (27 days) | | - | 539.4 | 200.5 | 1325.2 | |
| averages: | | | 6.98 | 20.0 | 7.43 | 49.1 | avg. flow = 2.46 L/s |

notes: - "L" means data logged before or after recording period.
- ~ static head means interpolated between measured values.
- [x] means value incorrect , anomalous or suspect.
1: data logged for only part of total operating period.
5: irradiance signal conditioning problem; signal corrected.
6: anomalous data; result not reliable.

Table X. Summary of field trial results for the month of August.

| date (1987) | recorded signals (No.) | (hrs) | static head (m) | insol-ation (MJ/m²) | pump time (hours) | volume pumped (m³) | events and notes |
|---|---|---|---|---|---|---|---|
| Aug. 1 | 3 | 24 | ~7.00 | 28.0 | 8.4 | [60.4] | note 6 |
| Aug. 2 | 3 | 24 | ~7.02 | 8.9 | 2.7 | 12.4 | |
| Aug. 3 | 3 | 24 | ~7.03 | 14.1 | 5.3 | 23.1 | |
| Aug. 4 | 3 | 24 | ~7.04 | 11.3 | 5.3 | 13.4 | |
| Aug. 5 | 3 | 24 | ~7.05 | 26.8 | 8.7 | 72.7 | |
| Aug. 6 | 3 | 16.6 L | 7.06 | 26.3 | 8.4 | 66.3 | note 5 |
| Aug. 7 | 3 | 24 | ~7.06 | 19.6 | 8.1 | 39.7 | |
| Aug. 8 | 3 | 24 | ~7.07 | 23.1 | 9.0 | 62.3 | |
| Aug. 9 | 3 | 24 | ~7.08 | 7.4 | 0.3 | 0.5 | |
| Aug.10 | 3 | 24 | ~7.09 | 21.3 | 7.8 | 52.1 | |
| Aug.11 | 3 | 24 | ~7.10 | [17.2] | 8.7 | 69.0 | note 6 |
| Aug.12 | 3 | 24 | ~7.11 | [21.5] | 8.9 | 71.8 | note 6 |
| Aug.13 | 3 | 24 | ~7.12 | 20.7 | 7.8 | 53.7 | |
| Aug.14 | 8 | L[15.3] | 7.12 | [5.2] | 3.2 | 8.4 | note 1 |
| Aug.15 | 8 | 24 | ~7.12 | 6.8 | 0.4 | 0.9 | |
| Aug.16 | 8 | 24 | ~7.13 | 13.2 | 5.6 | 26.9 | |
| Aug.17 | 8 | 24 | ~7.13 | 13.4 | 5.0 | 15.5 | |
| Aug.18 | 8 | 20.0 L | ~7.14 | [14.0] | 8.5 | 45.2 | note 6 |
| Aug.19 | 3 | 24 | ~7.14 | 19.7 | 8.2 | 41.0 | |
| Aug.20 | 3 | 24 | ~7.15 | 24.2 | 8.2 | 54.4 | |
| Aug.21 | 3 | 24 | ~7.16 | 17.2 | 8.0 | 34.8 | |
| Aug.22 | 3 | 24 | ~7.16 | 13.3 | 7.4 | 29.0 | |
| Aug.23 | 3 | 24 | ~7.17 | 21.6 | 7.2 | 52.4 | |
| Aug.24 | 3 | 24 | ~7.18 | 26.5 | 8.2 | 72.5 | |
| Aug.25 | 3 | 18.4 L | 7.18 | 20.0 | 6.8 | 49.5 | |
| Aug.26 | 8 | 24 | ~7.20 | 21.4 | 7.8 | 48.5 | |
| Aug.27 | 8 | 17.0 L | 7.22 | 23.2 | 8.2 | 53.7 | check calibrations |
| Aug.28 | 3 | 24 | 7.01 | 18.7 | 6.8 | 41.4 | adjust discharge |
| Aug.29 | 3 | 24 | ~7.01 | 17.8 | 5.5 | 34.4 | |
| Aug.30 | 3 | 24 | ~7.01 | 20.9 | 7.4 | 46.7 | |
| Aug.31 | 3 | 24 | ~7.01 | 4.1 | 0.4 | 0.4 | |
| Sep. 1 | 3 | 24 | ~7.02 | 11.1 | 3.6 | 10.5 | |
| Sep. 2 | 0 | 0 | 7.02 | ? | [0] | [0] | dismantle system |
| totals: | (27 days) | | - | 472.6 | 168.1 | 1008.7 | |
| averages: | | | - | 7.10 | 17.5 | 6.23 | 37.4 | avg. flow = 1.67 L/s |

notes: - "L" means data logged before or after recording period.
- ~ static head means interpolated between measured values.
- [x] means value incorrect , anomalous or suspect.
1: data logged for only part of total operating period.
5: irradiance signal conditioning problem; signal corrected.
6: anomalous data; result not reliable.